Developmental Biology 396 (2014) 121–135

Contents lists available at ScienceDirect

Developmental Biology

journal homepage: www.elsevier.com/locate/developmentalbiology

Spatial and molecular cues for cell outgrowth during *C. elegans* uterine development

Srimoyee Ghosh [a,b], Paul W. Sternberg [a,b,*]

[a] Division of Biology and Biological Engineering, California Institute of Technology, Pasadena, CA 91125, USA
[b] Howard Hughes Medical Institute, California Institute of Technology, Pasadena, CA 91125, USA

ARTICLE INFO

Article history:
Received 4 June 2014
Received in revised form
19 September 2014
Accepted 22 September 2014
Available online 2 October 2014

Keywords:
Trio
Nav
Rab
C. elegans
Cell outgrowth
Nuclear migration

ABSTRACT

The *Caenorhabditis elegans* uterine seam cell (utse) is an H-shaped syncytium that connects the uterus to the body wall. Comprising nine nuclei that move outward in a bidirectional manner, this synctium undergoes remarkable shape change during development. Using cell ablation experiments, we show that three surrounding cell types affect utse development: the uterine toroids, the anchor cell and the sex myoblasts. The presence of the anchor cell (AC) nucleus within the utse is necessary for proper utse development and AC invasion genes *fos-1, cdh-3, him-4, egl-43, zmp-1* and *mig-10* promote utse cell outgrowth. Two types of uterine lumen epithelial cells, uterine toroid 1 (ut1) and uterine toroid 2 (ut2), mediate proper utse outgrowth and we show roles in utse development for two genes expressed in the uterine toroids: the RASEF ortholog *rsef-1* and Trio/*unc-73*. The SM expressed gene *unc*-53/NAV regulates utse cell shape; ablation of sex myoblasts (SMs), which generate uterine and vulval muscles, cause defects in utse morphology. Our results clarify the nature of the interactions that exist between utse and surrounding tissue, identify new roles for genes involved in cell outgrowth, and present the utse as a new model system for understanding cell shape change and, putatively, diseases associated with cell shape change.

Introduction

Understanding the mechanisms necessary for one cell's behavior can shed light on the genetic inputs necessary for organogenesis. Many growing cells reorganize their cytoskeletons and respond to attractive and repulsive cues to reach their final developmental destinations, promoting tissue development, as seen with cells in the vertebrate neural crest, the *Drosophila* caudal visceral mesoderm, and neural growth cones (Hall, 2009; Le Douarin and Kalcheim, 1999; Theveneau and Mayor, 2012; Bronner and LeDouarin, 2011; Kadam et al., 2012; Vitriol and Zheng, 2012; Cajal and Ramón, 1890; Gomez and Zheng, 2006). *C. elegans* is a useful model for understanding these types of cell behavior. For instance, the TLX/*tailless* ortholog *nhr-67* controls *C. elegans* male gonad linker cell migration (Kato and Sternberg, 2009), and is well characterized in the developing *Drosophila* nervous system (Pignoni et al., 1990), and in mouse neural stem cell generation (Zhang et al., 2008). Netrin/UNC-6 and its receptor, UNC-40 were also discovered in *C. elegans* (Hedgecock et al., 1987, 1990; Ishii et al., 1992) and are key attractive and repulsive cues necessary for growth cone outgrowth. Therefore, characterizing the cell biology of *C. elegans* tissues has had broader implications in understanding mechanisms of other organism's development.

The *Caenorhabditis elegans* uterine seam cell (utse) is a syncytium that undergoes a striking outgrowth and nuclear migration during its development. Given the power of genetics in *C. elegans*, we thought that the utse offered an excellent system to study novel molecular mechanisms involved in cell outgrowth, cell shape change and syncytial cell biology.

Studying cell outgrowth and shape change provides valuable insights for a variety of systems. Aside from its role in growth cone migration and metastatic cancers, cell outgrowth and cell shape change are also involved in wound healing, through the recruitment of keratinocytes that extend lamellipodia towards the wound site (Martin and Leibovich, 2005; Grinnell, 1992; Martin, 1997), as well during TGF-β signaling driven transformation of fibroblast cells to myofibroblasts (which form cytoplasmic filamentious apparatuses cells in the presence of the wound) (Gabbiani 2003; Gabbiani et al., 1971).

The utse is a syncytium formed by the fusion of nine cells. Several syncytiums exist in biology, including embryonic and adult musculature, and vertebrate placenta (Biressi et al., 2007; Robertson et al., 1990; Robertson et al., 1993; Cross, 2000). The fusion events that contribute to the creation of these tissues have been well

* Corresponding author.
E-mail addresses: sghosh@caltech.edu (S. Ghosh), pws@caltech.edu (P.W. Sternberg).

http://dx.doi.org/10.1016/j.ydbio.2014.09.028
0012-1606/

characterized, and thus studying the cell behavior of the utse can contribute to understanding the morphogenetic movements that these syncytiums undertake. For instance, after fusion of post-mitotic precursor cells that make up the syncytial layer of the placenta, the syncytioblast, this syncytial layer expands and flattens to form a layer of tissue between the mother and fetus (Cross, 2000). Genetic inputs that control this behavior are not characterized and the utse can act as a model to study syncytial movement. Furthermore, abnormal placental formation can result in a slew of diseases, including preeclampsia, and therefore information contributing to syncytium regulation can prove vital.

The utse is also a heterokaryon, since it results from the fusion of two cell types, uterine υ cells (defined below) and the anchor cell. Investigating utse cell biology can contribute to our understanding of heterokaryons, which occur broadly in biology. Some examples include their presence in fungi, such as in *Schizophyllum commune* where genes from two types of nuclei (SC3/SC4) come together to interact with one another transcriptionally (Schuurs et al., 1998); their involvement in cell reprogramming (the fusion of embryonic stem cells with somatic cells induces pluripotency) (Tada et al., 2001); their promotion of tumor proliferation (through fusion of tumor cells with non-tumorigenic cells) (Berndt et al., 2013); and their association with multiple sclerosis (fusion of bone marrow cells and cerebellar Purkinje cells in brain tissue of patients with multiple sclerosis) (Kemp et al., 2012).

Due to the unique characteristics of the utse being both a syncytium and a heterokaryon, and because its mechanisms for outgrowth are predominantly uncharacterized, we chose to study the molecular inputs involved in utse development. Specifically, we sought to determine which surrounding uterine cells play a role in utse development. Using laser ablation we identified four cell types involved in utse development: the anchor cell (AC), uterine toroid 1 (ut1), uterine toroid 2 (ut2), and the sex myoblasts (SMs). We show that genes involved in AC invasion have an additional role promoting utse cell outgrowth. ut1 and ut2 are epithelial cells that are part of the uterine lumen, and through a candidate RNAi based screen on genes expressed in these cells, we identified two genes that play roles in utse development: RASEF/*rsef-1* and Trio/*unc-73*. The SMs form the uterine and vulval muscles that laterally flank the utse, and we show roles for the SM localized gene, *unc-53*/NAV in utse outgrowth. These results identify both external and internal cues necessary for utse development and characterize genes that are candidates for the production of these cues.

Materials and methods

Strains and genetics

C. elegans were handled as described previously (Brenner, 1974). All strains used (listed in supplementary material Table S1) are derivatives of *C. elegans* wild-type strain (N2 Bristol).

RNAi experiments

RNAi was performed by feeding nematodes dsRNA-producing bacteria using standard procedures (Timmons et al., 2001) modified as follows. Overnight starter cultures were grown with 1 ml LB supplemented with 25 μg/ml carbenicillin and 12.5 μg/ml tetracycline inoculated with a bacterial colony containing a plasmid producing dsRNA targeting a gene of interest. Starter cultures were diluted 1:80 the next day, using 100 ul of starter culture in 8 ml LB containing 25 ug/ml carbenicillin. Cultures were grown between 6 and 8 h to OD_{600} ~0.5. 6 cm Petri plates containing NGM agar that had been dried for at least three days at room temperature were prepared by using sterile glass beads to spread 50 μl of 25 mM carbenicillin, and 1 mM IPTG in M9 on each plate. RNAi cultures were then transferred to 1.5 ml microcentrifuge tubes (1 tube/plate) and then spun at 5000 rpm for 5 min. The majority of the supernatant was removed leaving about 50 μl of liquid plus bacterial pellet. Pellets were then resuspended in this solution, and then spread using sterile glass beads on the NGM agar+carbenicillin+IPTG Petri plates described in the preceding step. Plates were grown at room temperature overnight, and, if not used immediately, were stored at 4 °C for no more than a week. On the day of the experiment, plates were pipetted with 50 μl of a 1:5 solution of 1 M IPTG:M9. Plates were then dried for 10 min near a Bunsen burner. Eggs were bleached onto RNAi plates and allowed to hatch and develop. Phenotypes were scored at the L4 lethargus stage. For RNAis used see Table S2.

Scoring utse phenotypes

Animals were scored using a wide-field epifluorescence microscope at young adult or L4 lethargus stage. Wild-type utse cell body length is between 300 and 400 μm, and distance between wild-type nuclei is between 250 and 350 μm. Animals were classified as abnormal if both the utse cell body and nuclear distance were 50 μm greater or less than that of the wild type range (i.e. an animal was still classified as abnormal if its cell body was within the wild-type range but its nuclear distance was not.) All abnormal animals in this publication fit within this criteria and some exhibit other defects, such as missing arms, abnormal shape, or holes in portions of the cytoplasm.

Transgenics

To make the *exc-9::mcherry* construct, 20 ng/μl of *exc-9::mcherry* plasmid (pBK162, *exc-9::mcherry* gateway plasmid, from M. Buechner, WBperson81) was injected into *unc-119*(*ed4*) with an *unc-119* rescue construct.

Ablations

Cell ablation experiments were performed as described (Bargmann and Avery, 1995). Dorsal uterine cells and uterine toroid cells were ablated at late L3; see Fig. 2B-B‴ and Fig. 3A. Anchor cells were ablated at early L4; see Figs. 2D–D″ and Fig. 4A. Sex myoblasts were ablated at L1, see Fig. 9 P,S,T. All ablated worms were scored between late L4 and L4 lethargus.

Results

Wild-type C. elegans utse behavior

The hermaphrodite uterus is composed of several different cell types (Fig. 1A). The uterus lies dorsal to the vulva, and is derived from the dorsal uterine (DU) and ventral uterine (VU) cell lineages (Fig. S1A; Kimble and Hirsh, 1979; Newman et al., 1996). The DU and VU lineages generate several different cell types, such as the dorsal uterine cell (du), which makes up the dorsal most portion of the uterus; uterine toroid (ut) cells, which line the uterine lumen; and the uterine-vulva (uv) cells, which connect the uterus to the vulva (Figs. 1A and F, 3A and 4A).

The utse attaches the uterus laterally to the body wall via the seam cells (Fig. 1A). The utse in *C. elegans* mid L4 hermaphrodite is shown in Fig. 1B. utse nuclei are marked with *egl-13::gfp,* which marks the υ cells (see below for definition), and *cdh-3::PH::mcherry,* which uses the phospholipase-C plekstrin-homology (PH) domain fused to mCherry to direct expression in the utse

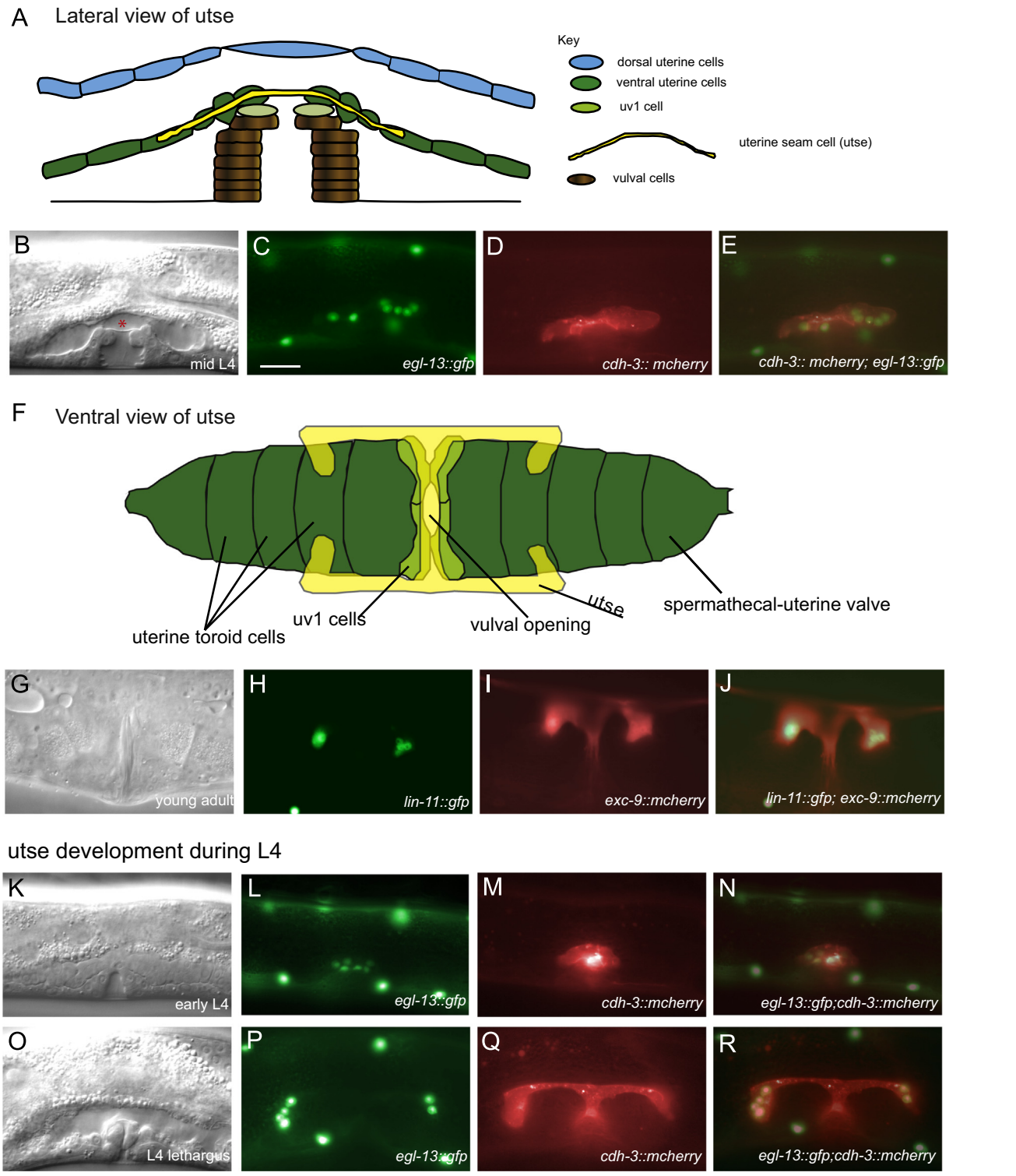

Fig. 1. Wild-type utse development (A) Lateral schematic of a mid L4 uterus. (B-E) utse development at mid L4. (B) mid L4 somatic gonad; utse is shown underneath red asterisk. (C) υ cell nuclei (hereafter referred to as utse nuclei) shown with egl-13::gfp. D) utse cell body marked with cdh-3::mcherry. (E) merge of C-D. (F) Ventral schematic of L4 lethargus uterus. (G-J) Ventral view of young adult uterus. (G) young adult somatic gonad. (H) utse nuclei (υ cell nuclei) marked with lin-11::gfp. (I) cell body marked with exc-9::mcherry. (J) merge of H-I. (K-R) utse nuclei marked with egl-13::gfp and cell body marked with exc-9::mcherry. (K-N) utse development at early L4, here nuclei (L,N) are clustered together and the cell body (M,N) has an ellipsoid shape. (O-R) utse development at L4 lethargus (O), here the cell body (Q,R) has elongated in an anterior-posterior manner and nuclei (P,R) have migrated to distal tips of utse. Scale bar, 100 μm.

cell body/plasma membrane (Fig. 1D and E; Ihara et al., 2011). At mid L4 (Fig. 1B–E) the utse is undergoing both cell outgrowth and nuclear migration and it will reach its final shape at L4 lethargus (Figs. 10–1R). The ventral view of the utse (Fig. 1F) highlights its H-shaped form, with the middle of the H lying above the vulval opening, and the two sides mediating a connection between the seam cells of the body wall and ut2 (Fig. 1F–J).

At late L3 stage, six of the VU granddaughter cells are induced via LAG-2-LIN-12 Notch-Delta signaling from the AC to become π cells (Fig. S1B and C; Newman et al., 1995). After these six π cells are

induced, they divide to make 12 π-progeny cells (Fig. S1C and D; Newman et al., 1996). Four of these 12 π-progeny cells become uv1 cells via EGF signaling (Fig. S1E; Chang et al., 1999) from the vulval vulF cells; the remaining eight will later fuse with one another and then with the AC to form the syncytial cell body of the utse by the mid fourth larval (L4) stage via the fusogen AFF-1 (Fig. S1F; Figs. 1K–N; Sapir et al., 2007). We will henceforth refer to the eight π-progeny cells that do not become uv1 and form the utse nuclei as υ (upsilon) cells. During early L4, as visualized in Fig. 2B–B″, the AC induces surrounding π cells but has not yet fused with these cells (since *cdh-3::PH::mcherry* expression is limited to the AC), and later in L4, as seen in Fig. 2C′-C″, the AC has fused with the π-progeny cells, the υ cells (*cdh-3::PH::mcherry* has spread throughout the entire utse cell body).

Over the next eight hours the utse cell body grows bi-directionally along the anterior-posterior axis, and the utse nuclei segregate into two groups (Fig. 2F″–F‴), migrate along the anterior posterior axis, and settle at the anterior/posterior edges of the utse cell body (Fig. 2H–H‴; Newman et al., 1996). The utse cell body extends ahead of its nuclei during development (Fig. 2E‴) indicating that separate mechanisms may be controlling these two behaviors; however, we observe defects in cell morphology associated with aberrant nuclear positioning (Fig. 3). Therefore, both aberrations in nuclear migration and cell outgrowth were used to characterize defective utse development (see Materials and Methods for specific criteria for scoring phenotypes).

Two genes have been previously characterized for their roles in proper utse cell elongation and nuclear migration: the LIM domain transcription factor *lin-11* and the SOX domain transcription factor *egl-13* (Newman et al., 1999; Hanna-Rose and Han, 1999; Cinar et al. 2003). Both *lin-11* and *egl-13* are involved in AC fusion with the utse, as well as induction of π cell fate, and their role in utse cell outgrowth/nuclear migration has been attributed to these behaviors. We wished to better understand the role of the AC in utse development, as well as identify cues from surrounding uterine cells acting on the utse.

Surrounding uterine cells have an effect on utse development

We hypothesized that interactions between the utse and its surrounding tissues would be necessary for proper utse development. To this end, we ablated surrounding uterine cells and observed subsequent effects on utse development (Fig. 3A). utse development was assessed by examining υ cell nuclei marked with nuclear-localized GFP driven by an *egl-13* promoter, and by examining utse cell bodies marked by *exc-9::gfp* translational fusion reporter. (Fig. 3B–I; Wendy Hanna-Rose personal communication, Tong and Buechner, 2008).

Without the presence of *egl-38*-dependent EGF signal necessary for uv1 cell fate, presumptive uv1 cells take on υ cells identities and fuse with the naturally occurring υ cells to form a wild-type utse with extra nuclei (Chamberlin et al., 1997). *cog-3/pnc-1* mutants lack the EGF signal necessary for uv1 fate and do not form uv1 cells, and these mutants show no defects in utse cell fate specification or morphology (Huang and Hanna-Rose, 2006). We therefore infer that uv1 cells do not affect utse development and chose not to ablate these cells.

We hypothesized that the du cell could potentially be pushing downward on the utse, causing it to stretch outward. However, du ablation had no effect on utse cell behavior (0%, $n=26$). Next, we tested the effect of the surrounding uterine toroid cells on utse development by ablating each set of uterine toroid cells. Cell ablations were performed at early L4 stage. At this stage the four nuclei found within each toroid cell were easily visualized, lumen formation had not occurred (uterine toroid lumen formation occurs at mid L4), and utse development had not commenced (Figs. 2B–B‴, 3A, Newman et al., 1996). Fig. 3A shows the progression of ut1 ablation. Animals were scored at L4 lethargus, approximately 6–8 h after ablation. Mock ablations with exposure to anesthetic used (3 mM levamisole) had no effect on utse development (0% defect, $n=10$; Table 1; Fig. 3B and C). Ablations of uterine toroid 1 (ut1) or uterine toroid 2 (ut2) caused defects in utse development (Fig. 3D–G, Table 1). 88% of ut1-ablated worms ($n=26$) showed defects in nuclear migration (compare Fig. 3D to B) and had utse cell bodies that were both shorter than wild type and missing portions (compare Fig. 3E to C). ut2 is the second most proximal toroid cell to the utse, and is the last toroid cell with which the utse makes contact (Newman et al., 1996). 91% of ut2 ablated worms showed defects ($n=12$, Table 1) including reduced distance between utse nuclei in ut2 ablated worms (compare Fig. 3F to B), and a shorter cell bodies containing missing portions and vacuoles (compare Fig. 3G to C). Ablation of the next most distal ut cell, ut3, which has no direct contact with the utse, caused no defects in nuclear migration or cell outgrowth (Compare Fig. 3H I to B and C). We conclude that ut1 and ut2 are involved in utse development.

Internal signals involved in utse development

Since the AC fuses with the utse during early L4 (Fig. 2C–C‴; Sapir et al., 2007) we asked if transcription within the AC-derived nucleus was necessary for utse development. We performed the cell ablations after mid L4, the stage at which the AC had already induced π cells, fused with the υ cell nuclei, and its nucleus could be easily identified due to its position in a unique plane of focus relative to other nuclei in the worm (Figs. 2D–D‴, Fig. 4A; Félix and Sternberg, 1996). This timing of the ablation avoided any secondary effects that could have resulted from earlier ablations of the AC. AC nuclear ablation caused defects in utse development (86% abnormal, $n=23$). utse nuclei were clustered together in AC nuclear ablated worms (compare Figs. 3B to 4B) and utse cell bodies were short and deformed (compare Figs. 3C to 4C). As a control, we ablated υ cell nuclei to determine if defects were AC nuclei specific or a result of ablating any nucleus in the utse. Ablation of υ cell nuclei resulted in wid-type phenotypes (0% defects, $n=6$; Table 1). Since we specifically ablated the AC nucleus after fusion, we also eliminated the possibility that the AC cytoplasm was contributing to utse outgrowth. The finding that the AC nucleus is necessary for utse development suggests that transcription factors expressed in the nucleus are required, as addressed below.

AC fusion is necessary for utse development

To verify if the AC was necessary for utse development, we observed utse development in the absence of AC-utse fusion. During early L4, the AC fuses with the utse via the fusogen *aff-1* (Sapir et al., 2007). *aff-1*(*RNAi*) treatment resulted in a clear failure of AC fusion as assayed by the *cdh-3::PH::mcherry; egl-13::gfp* marker initially expressed in the AC (Fig. 5A–C; Table 2) and defective utse cell outgrowth, as assayed by *exc-9::gfp* (Fig. 5D). Even though there is no AC fusion in these worms, the υ cell nuclei still migrated outward, albeit at a distance shorter than of wild type (Fig. 5C).

To rule out that these defects result from global issues in cell fusion, we examined the function of *eff-1,* which is involved in heterologous fusion events in *C. elegans* (Podbilewicz et al., 2006). Worms treated with *eff-1*(*RNAi*) showed a small but statistically significant defect in utse nuclear migration (11%, $n=43$, *P*-value 0.0087; Table 2E) and no defects in utse cell outgrowth (0%, $n=7$; Table 2E).

AC invasion genes act during L4 to affect utse development

During late L3, the AC forms protrusions that span the basement membrane between the uterus and the vulva to invade the vulval epithelium (Sherwood and Sternberg, 2003). Because the AC changes its shape during protrusion formation, we hypothesized that genes

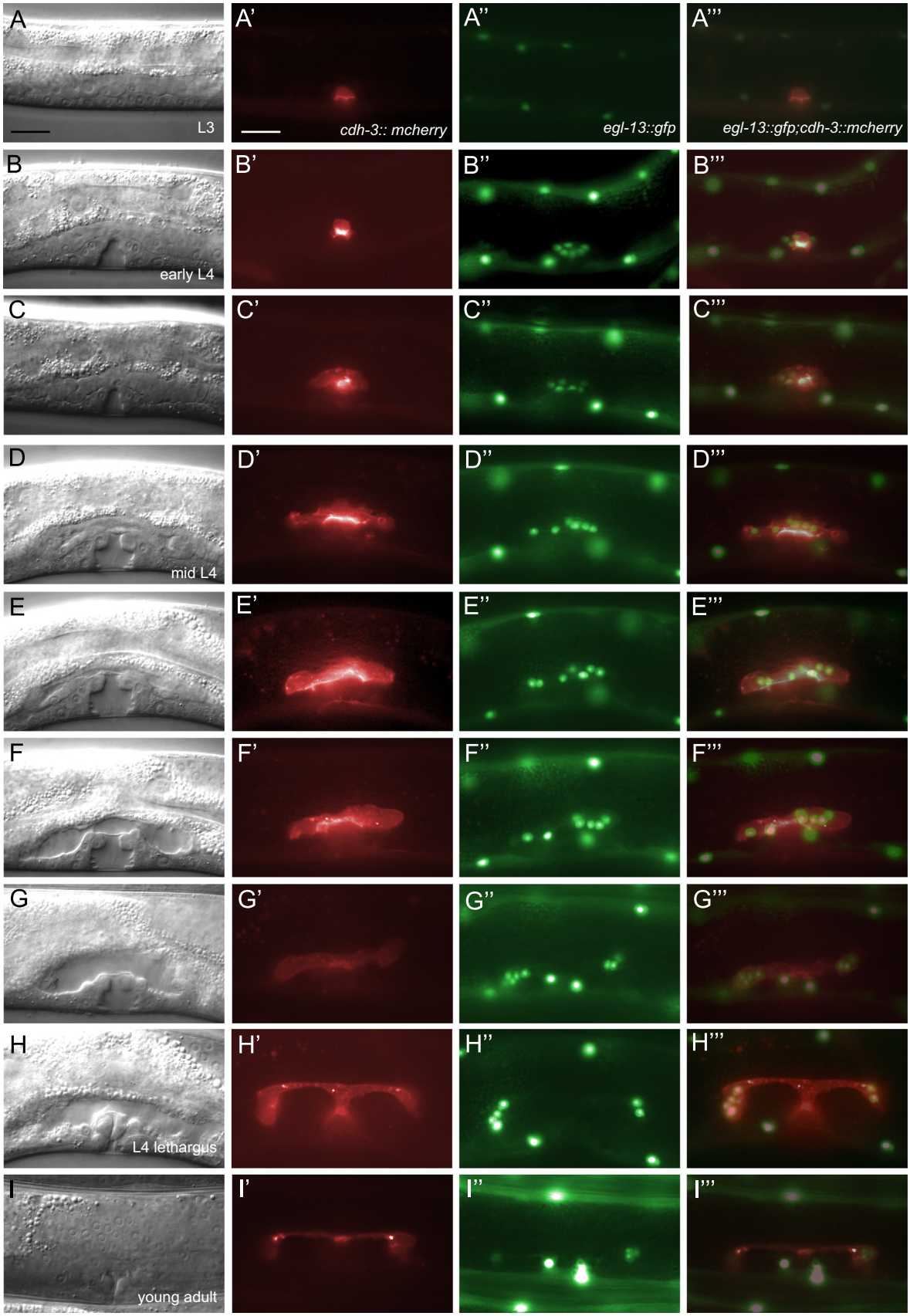

Fig. 2. utse development from L3 to young adult Sections (A) through (I) are in chronological order from earliest (L3) to latest (young adult). Each section includes a Nomarski image, expression of the *cdh-3::mCherry* marker in the cytoplasm of the AC and later the utse, expression of the *egl-13::gfp* marker in the nuclei of the υ cells and later the utse cell; and a merge of *mCherry* and *gfp* expression. Nuclei are marked with *egl-13::gfp* and cell body is marked with *cdh-3::mcherry*. 10 worms were scored for each stage, and most representative image is shown. (A-A"') L3, AC invasion, pi cells have not been specified. (B-B"') early L4, pi cells are specified by the anchor cell. (C-C"') fusion between υ cell nuclei an anchor cell. (D-D"') mid L4, cell body outgrowth has commenced, nuclei are rearranging and begun migrating slightly. (E-G"') cell body outgrowth and continues, with outgrowth occurring at a faster rate than nuclear migration. (H-H"') L4 lethargus, nuclear migration and cell outgrowth has completed, and the utse has taken its final shape. (I-I"') Young adult, utse cell body will maintain this shape until egg-laying occurs. Scale bar, 100 μm.

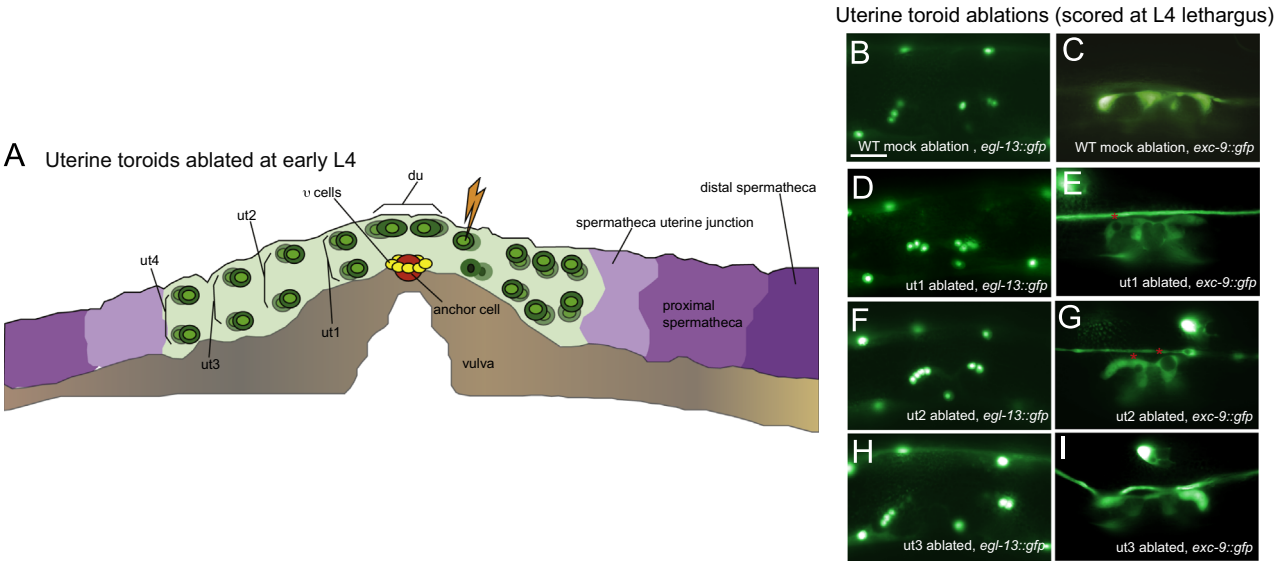

Fig. 3. Uterine toroid ablations. (A) schematic of early L4 uterus. Lightning bolt indicates ablation of ut1 and borderless cells indicate cell death. (B) completed nuclear migration in mock ablation worm (nuclei marked with *egl-13::gfp*). (C) completed utse cell outgrowth in mock ablated worm (cell body marked with *exc-9::gfp*). (D-E) ut1 ablated worms. (D) shorter nuclear migration. (E) short and perforated cell body. (F-G) ut2 ablated worms. (F) shorter nuclear migration. (G) short and perforated cell body (see asterisks). (H-I) ut3 ablated worms (H) nuclei distance in ut3 ablated worms is comparable to wild-type, C. (I) utse cell body in ut3 ablated worm looks similar to wild-type, E. Scale bar, 100 μm.

Table 1
Uterine cell ablations.

Genotype	% Defect	n	*P*-value
mock ablation	0	10	
du ablated	0	26	
ut1 ablated(nuclear)	84.6	13	< 0.0001
ut1 ablated (cell membrane)	92.3	13	< 0.0001
ut1 ablated (total)	88.5	26	< 0.0001
ut2 ablated(nuclear)	85.7	7	< 0.0001
ut2 ablated (cell membrane)	100	5	< 0.0001
ut2 ablated (total)	91.67	12	< 0.0001
ut3 ablated(nuclear)	0	7	
ut3 ablated (cell membrane)	0	4	
ut3 ablated (total)	0	11	
Anchor cell ablated (nuclear)	83.3	18	< 0.0001
Anchor cell ablated (cell membrane)	100	5	< 0.0001
Anchor cell ablated (total)	86.9	23	< 0.0001
Sex Myoblasts	90	10	< 0.0001
υ cell nuclei	0	6	

Uterine toroid 1, uterine toroid 2, anchor cell and sex myoblasts are necessary for utse development. All phenotypes were scored at L4 lethargus or young adult. P-values were were calculated in comparison with wild type cdh-3::mcherry; egl-13::worms using Fisher's exact test.

involved in this process can also contribute to utse cell shape change. During AC invasion, the *c-fos* transcription factor ortholog *fos-1* promotes expression the zinc metalloprotease *zmp-1*, the protocadherin *cdh-3*, the zinc finger protein *egl-43*, the hemicentin extracellular matrix protein gene *him-4*, and lamillopodin/*mig-10*; the activities of these genes induce the AC to form ventrally directed protrusions that breach the basement membrane (Fig. 6A; Sherwood et al., 2005; Hwang et al. 2007; Wang et al., 2014). RNAi against the AC invasion genes resulted in defects in utse development (Table 2E; Fig. 6B–D; F–H; J –L; N–P; R–T; V–X), supporting our hypothesis that genes involved in AC protrusion formation also affect utse development.

Each of these genes are expressed within the AC during invasion (Sherwood et al., 2005; Hwang et al. 2007; Wang et al., 2014). Since the AC nucleus is necessary for utse development, we asked if these genes were transcriptionally active throughout L4 and were present in the utse. We observed that transgene reporters for *fos-1, egl-43, zmp-1, cdh-3* and *mig-10* were all expressed in the utse at L4 lethargus or young adult (Figs. 6E, I, M, U and Y) consistent with a role in utse development. *mig-10* is also expressed in uterine toroids in L4 (Fig. 6Y), and could be acting on the utse via signals from the uterine toroids, or internally like the other invasion genes. *him-4* encodes the extracellular matrix protein hemicentin, which assembles into polymers at areas of cell contact to help mediate the connection between the uterus and the hypodermis (Newman et al., 1995; Vogel et al., 2006). As it is necessary for mediating cell-cell interactions, and is expressed ventral to the utse (Fig. 6Q) it is not surprising that lack of hemicentin in *him-4*(*RNAi*) also results in utse defects even though *him-4* is not expressed in the utse (Fig. 6Q).

fos-1(*RNAi*) and *egl-43*(*RNAi*) treated worms showed severe defects not only in utse development but in somatic gonad development (data not shown). This effect was partially due to their involvement in π cell induction (Oommen and Newman, 2007; Rimann and Hajnal, 2007), which made nuclear migration difficult to score. The majority of *fos-1*(*RNAi*) and *egl-43*(*RNAi*) treated worms did not form π or υ cells (Table 2E) but those shown in Fig. 6 and Table 2E were animals in which π and subsequently υ cell induction occurred. Both *fos-1* and *egl-43* are expressed in the utse at late L4 and young adult stages, indicating that they likely also act in the utse, and defective phenotypes from RNAi treatment against these genes is not wholly due to lack of π cell production.

Due to the presence of utse defects upon knockdown of AC invasion genes, as well expression of the invasion genes within and surrounding the utse cell body, we believe to have discovered a new role for the AC in uterine development.

Molecular signals from ut1 and ut2 affect utse development

After determining that the uterine toroid cells (specifically ut1 and ut2) play a role in utse development we examined underlying genetic requirements. To this end, we generated a list of 37 genes expressed in the uterine toroids through a WormBase expression pattern search. We performed RNAi against these candidates and screened for defects in utse development (see Table 2A). Defects resulting from these

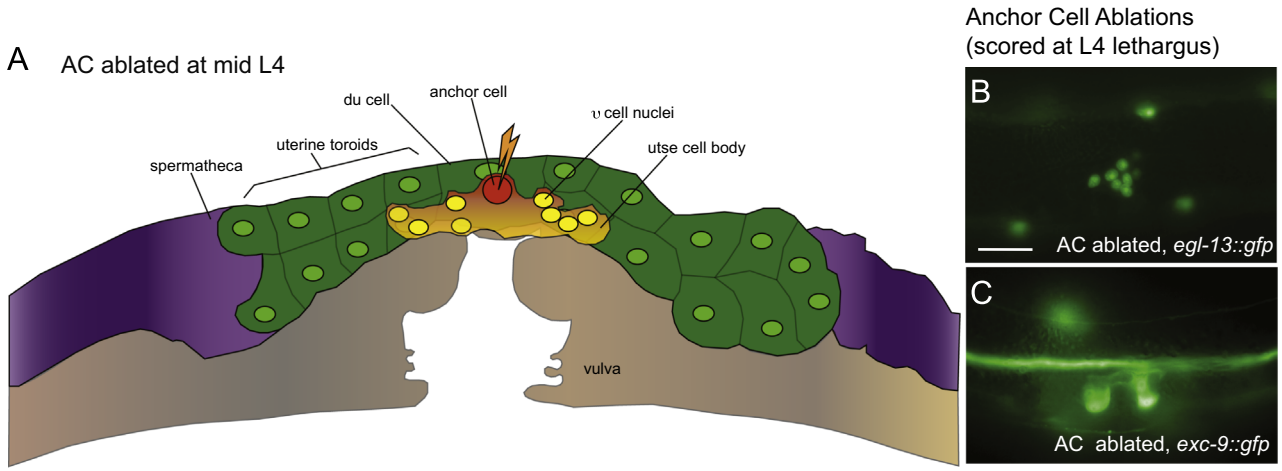

Fig. 4. AC ablations (A) schematic of mid L4 uterus. Lightning bolt indicates the point at which AC nucleus was ablated. (B-C) images of worms with anchor cell ablated. (B) nuclei are clustered together, migration has not occurred. (C) cell body has not undergone cell outgrowth. Scale bar, 100 μm.

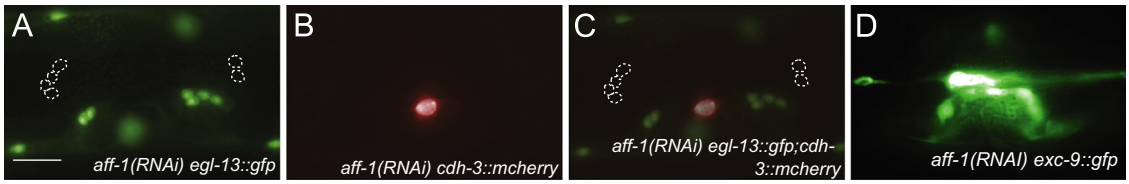

Fig. 5. AC fusion and its role in utse development (A-C) utse cell body is marked with *cdh-3::mcherry* and utse nuclei are marked with *egl-13::gfp*. (A-D) *aff-1*(*RNAi*) treated worms (A,C) shorter nuclear migration, cartoon in *F* and *C* indicate wild-type nuclear spacing. (B,C) AC has not fused with υ cells in *aff-1* (*RNAi*) treated worms; however, nuclear migration has continued, though at a shorter distance comparable to wild-type. (D) shorter utse cell body (marked with *exc-9::gfp*) upon treatment with *aff-1*(*RNAi*). Scale bar, 100 μm.

genes would be significant since their expression (and potentially site of action) in the uterine toroids would bolster our finding that the presence of the uterine toroids affect utse development.

Of the 37 genes, 7 exhibited extremely significant defects in utse development (Table 2A): helicase *dog-1,* the serine carboxypeptidase *F41C3.5*, the phosphatase *gsp-1,* the EGF vulval induction gene *lin-3,* the cell fusion annexin *nex-1,* the divergent Rab GTPase RASEF/*rsef-1* (formerly known as *tag-312*), and the GNEF (guanine nucleotide exchange factor) Trio-like protein *unc-73* (Youds et al., 2007; Saleh et al., 2006; Hristova et al., 2005; Rutledge et al., 2002; Hill and Sternberg, 1992, 2004; Satoh et al., 2000; Daigle and Creutz, 1999; Shaye and Greenwald, 2011; Schmidt et al., 2009; Stringham et al., 2002; Wu et al., 2002). We focused on two of these genes: *rsef-1,* due to its uncharacterized nature, and *unc-73,* due to the high frequency and severity of utse defects from RNAi knockdown of this gene (Fig. 9A–F).

rsef-1 is the *C. elegans* ortholog of RASEF (Wormbase website, 2014), a potent tumor suppressor and lung cancer biomarker (Oshita et al., 2013). It is necessary for PLM axon growth and is a known *C. elegans* spermatheca and spermatheca-uterine junction (sujn) marker (Chen et al., 2011). Exposure to *rsef-1*(*RNAi*) caused defects both in utse nuclear migration (Fig. 7E) as well as cell outgrowth (Fig. 7F). *rsef-1*(*RNAi*) also caused problems in uterine lumen formation (Fig. 7D), suggesting that the site of action is in the uterine toroids. To examine *rsef-1* expression we used a transcriptional fusion of *rsef-1* (Mounsey et al., 2002). Expression is absent during early and mid L4 stages, but is present both in the spermatheca and spermathecal-uterine junction at L4 lethargus (Fig. 7G), and in the uterine toroids at young adult stage (Fig. 7H and J). We observed phenotypic consequences of *rsef-1* silencing in the utse/uterine toroids prior to detecting expression of the *rsef-1::gfp* reporter, so we are likely missing some component of its expression.

Rab GTPases affect utse development

rsef-1 is largely uncharacterized and its upstream and downstream effectors are unknown. Using software that computationally predicts interactions between genes (geneorienteer.org; Zhong and Sternberg, 2006), we performed an RNAi screen against 14 of the top 15 predicted *rsef-1* interactors (Table 2B). (RNAi against *Y69H2.2* resulted in an absence of UTSE nuclei, data not shown.) RNAi treatment against three genes caused defects in utse development: the transcription factor *athp-1,* and two Rab GTPases, *rab-1* and *rab-11.1* (Fig. 8D - G, U- X). *athp-1* has been shown to affect nuclear migration potentially through the SUN/KASH pathway (S.G., unpublished observations).

RNAi against *rab-1* and *rab-11.1* resulted in severe defects (Fig. 8D–G, U–X). *rab-1* is expressed in several cell types including the uterine toroids (Fig. 8B). As *rsef-1* encodes a Rab family protein, we asked whether other Rab GTPases also affect utse development. Strikingly, of 21 tested, six Rab GTPases showed defects in utse development (Table 2C; Fig. 8D–X). These Rab GTPases are involved in several parts of the cell trafficking pathway including vesicle trafficking between the ER and the Golgi (*rab-1, rab-6, rab-10*), transport to the early endosome (*rab-5* and *rab-10*) and transport from the early endosome to the recycling endosome (*rab-11.1*) (Fig. 8C, Nishimura and Sasaki, 2008; Chen et al., 1993; Martinez et al., 1994). Since Rab GTPases are expressed globally, site of action experiments will be necessary to determine whether these Rab proteins exert their effects on utse development by acting in the toroids, the utse, elsewhere, or in multiple tissues.

unc-73 regulates the environment of utse

unc-73 encodes a Rho GNEF related to the mammalian Trio protein (Steven et al., 1998), which regulates cell outgrowth, cell

Table 2
RNAis tested on utse.

Genotype	% Defect	N	*P*-value
empty vector RNAi	0.97	103	
A) genes expressed in the uterine toroids			
C25A1.5	0	20	1
cdh-4	0	11	1
ceh-24	8	25	0.1
ckb-2	0	20	1
cog-1	9	11	0.18
dcar-1	14	7	0.12
dog-1	50	20	< 0.0001
egl-36	0	10	1
F22G12.5	0	10	1
F33H2.3	0	10	1
F41C3.2	30	10	0.002
F41C3.5	37	46	< 0.0001
gly-2	0	4	1
gsp-1	38.5	39	< 0.0001
hex-2	0	21	1
homt-1	0	10	1
inx-11	0	24	1
inx-8	0	14	1
lin-3	37.5	24	< 0.0001
mls-1	0	20	1
nck-1	0	10	1
nex-1	50	28	< 0.0001
nhr-111	0	10	1
nhx-3	10.5	19	0.06
osm-9	15.4	13	0.03
pha-4	0	3	1
plc-3	0	10	1
rsef-1	66.7	18	< 0.0001
sca-1	3.7	27	1
ser-2	21.4	14	0.01
tag-24	8.3	12	0.2
tdc-1	0	26	1
tyr-2	0	25	1
unc-73	82	50	< 0.0001
unc-94	17.4	23	0.004
W01A11.1	12.5	8	0.14
Y45F10C.2	0	11	1
B) *rsef-1* predicted interactors*			
athp-1	40	20	< 0.0001
cdc-42	0	20	1
ced-10	0	13	1
F33A8.4	5.9	17	0.26
F55G1.13	9.5	21	0.07
let-502	0	10	1
let-60	9.1	11	0.18
rab-1	53	17	< 0.0001
rab-11.1	90.6	32	< 0.0001
rap-1	5	20	0.3
rap-2	0	10	1
ras-1	0	9	1
spt-5	20	20	0.002
tag-336	0	9	1
C) RabGTPases			
C56E6.2 (*rab-6* homolog)	0	20	1
F11A5.3 (*rab-2* homolog)	0	14	1
rab-1	52.9	17	< 0.0001
rab-10	95.5	22	< 0.0001
rab-11.1	90.6	32	< 0.0001
rab-14	0	27	1
rab-19	0	9	1
rab-2	33.3	9	0.001
rab-21	0	15	1
rab-28	0	24	1
rab-30	0	2	1
rab-3	0	10	1
rab-33	0	10	1
rab-35	0	10	1
rab-37	0	13	1
rab-39	0	14	1
rab-5	70.8	24	< 0.0001
rab-6.1	40	20	< 0.0001
rab-6.2	68.2	22	< 0.0001
rab-7	28.6	7	0.01
rab-8	18.2	11	0.02
D) *unc-73* and *unc-53* downstream genes			
cdc-42	0	20	1
ced-10	0	13	1
egl-15	79	19	< 0.0001
mig-2	0	10	1
pkc-1	30	30	< 0.0001
rho-1	94.1	17	< 0.0001
sem-5	16	25	0.0051
unc-13	50	24	< 0.0001
unc-53	73.1	52	< 0.0001
unc-64	50	30	< 0.0001
unc-71	25	8	0.01
E) genes involved in Anchor Cell fusion and invasion			
aff-1	67.9	28	< 0.0001
aff-1 cell fusion defective	100	11	< 0.0001
cdh-3	38.5	26	< 0.0001
eff-1	11.1	43	0.01
eff-1 cell outgrowth	0	7	1
egl-43	100	29***	< 0.0001
fos-1	100	15**	< 0.0001
him-4	42.9	49	< 0.0001
mig-10	86.7	15	< 0.0001
zmp-1	62.5	24	< 0.0001

*genes in this section have Gene Orienteer scores that designate computational interaction between *rsef-1*.
Phenotypes were scored at L4 lethargus. *P*-values were calculated in comparison to empty vector (RNAi) using Fisher's exact test.

** 38 additional worms were scored but had no pi cell nuclei.
*** 52 additional worms were scored but had no pi cell nuclei.

migration and cytoskeletal rearrangements (Seipel et al., 1999). We observed that 82% of *unc-73*(*RNAi*) (n= 50) treated worms showed defects such as a thick, truncated utse cell bodies (Fig. 9B and C) and nuclei that failed to segregate into two groups and instead were linearly arranged (Fig. 9A and C).

We next examined the expression pattern of *unc-73* in the uterus using existing *unc-73* reporters. *unc-73* exists in eight isoforms, which are as follows: *unc73a, unc-73b, unc-73c1, unc-73c2, unc-73f, unc-73d1, unc-73d2 and unc-73e*) (Steven et al., 2005). Of these different isoforms, combinations of four were reported to be expressed in the uterine epithelium at late L4 (*unc-73a,b::gfp* and *unc-73d::gfp*) (Ziel et al., 2009). *unc-73a,b::gfp* was expressed in the vulva at early L4 (specifically the vulE and vulF cells) and later in the uterine toroid4/spermatheca-uterine junction at mid and late L4 (data not shown). The *unc-73d::gfp* construct is detectable in ut2 in early L4 (Fig. 9D), ut1 and ut2 and the utse at mid L4 (Fig. 9E) and in both the uterine toroids and the utse by L4 lethargus (Fig. 9F). Though *unc-73a,b::gfp* and *unc-73d::gfp* are predominantly expressed in the gonad, they are also expressed in other tissues, such as the pharynx and certain neurons. This, combined with the fact that the expression patterns of *unc-73c* and *unc-73f* have not been characterized, precludes a conclusion about its site of action.

We next identified genes downstream of *unc-73* that affect utse development. *unc-73* encodes a guanine nucleotide exchange factor required for activating Rho and Rac GTPases (Steven et al., 1998). The N-terminal RhoGEF-1 domain activates the Rac family of GTPases (Wu et al., 2002; Steven et al., 1998; Kubiseski et al., 2003) whereas the C-terminal RhoGEF-2 domain activates the RhoGTPase *rho-1* (Spencer et al., 2001). *unc-73d*, an isoform that contains the RhoGEF2 domain (Ziel et al., 2009) responsible for activating RHO-1 is expressed in ut1, ut2 and the utse. We thus tested the *C. elegans* ortholog of RHO-1, *rho-1*, and observed significant defects in utse development (94% defects cause defects *rho-1*(*RNAi*), *n*= 17,

Table 2D.) *let-502,* a Rho-binding serine-threonine kinase, is a downstream effector of *rho-1*, but does not have an effect on utse development (0% defects, $n=10$, see Table 2D); however, another downstream effector of *rho-1, unc-13,* may play a role (50% *unc-13* (*RNAi*) caused defects, $n=24$; Table 2D) (Spencer et al., 2001; McMullan et al., 2006). *unc-13* is a target of diacyl glycerol (DAG) signaling (Lackner et al., 1999), a pathway downstream of *rho-1* necessary for vesicle release. One of *unc-13*'s downstream effectors, *unc-64*/syntaxin, also affected utse development (50% *unc-64*(*RNAi*) caused defects, $n=30$; Table 2D). Other members of the DAG pathway, such as *pkc-1*, a serine-threonine kinase, too yield utse defects (30% *pkc-1*(*RNAi*) caused defects, $n=30$; Table 2D). (Note RNAi for *dgn-1/dystroglycan,* another downstream effector, was unavailable and therefore not tested.) These data suggest that UNC-73 acts on the utse by activating RHO-1, which then activates UNC-13 and potentially induces release of a chemoattractant through vesicle release via the DAG pathway.

The unc-73 interactor, unc-53, affects utse development via the SMs

unc-73 acts together with *unc-53*/NAV and *unc-71* promote guidance of SMs (uterine and vulval muscle progenitor cells) in the absence of the gonad (Branda and Stern, 2000; Chen et al., 1997; Marcus-Gueret et al., 2012; Siddiqui, 1990; Wightman et al., 1997). *unc-53* is a cytoskeletal binding protein related to the mammalian NAV1 protein (neuronal navigators) (Maes et al., 2002). RNAi knockdown of *unc-53* resulted in high frequency of defects (73% of *unc-53*(*RNAi*) ($n=52$) that were phenotypically similar to defects caused by *unc-73*(*RNAi*) (Table 2D). Specifically, *unc-53* (*RNAi*) treated animals exhibit a thick, truncated utse cell body (Figs. 9H–I) and nuclei are linearly arranged (Figs. 9G, I). *unc-71* (*RNAi*) had slight utse defects (25%, $n=8$). Since *unc-73*(*RNAi*) and *unc-53*(*RNAi*) exhibit stronger and more penetrant phenotypes, we infer that these two genes work together in utse development. *unc-73* and *unc-53* work together without *unc-71* to direct posterior outgrowth of the excretory canal, axonal guidance and outgrowth of PLM neurons, and growth cone guidance along the ventral nerve cord (Marcus-Gueret et al., 2012; Siddiqui, 1990; Wightman et al., 1997).

We determined the *unc-53* expression pattern using a reporter containing its full length promoter (*pABunc-53::gfp;* Stringham et al., 2002). Expression was present in the sex myoblasts (SMs) (Fig. 9K) as well as the vulval and uterine muscles they generate (Fig. 9K, M, O). The SMs laterally flank the utse from L3 onwards and generate the uterine and vulval muscles also known as the sex muscles (Fig. 9J, L, N; Sulston and Horvitz, 1977). Since *unc-53* expression was limited to the SM lineage, we investigated the role of the SMs (and their descendants, the uterine and vulval muscles) in utse development via cell ablation. The SMs originate from the M cell, and migrate to the uterine (Sulston and Horvitz, 1977). We ablated the M cell in the L1 larval stage (Fig. 9P), and then observed the utse at L4. In the absence of the SMs, the utse cell body exhibits abnormal morphology and expands beyond its normal position (Fig. 9S, T, Table 1). Defective utse development occurs in the absence of other genes localized to the SMs, such as treatment the FGF receptor *egl-15*(*RNAi*) (78.9% defect, $n=19$), substantiating our hypothesis that the SMs play a role in utse development. We conclude that the presence of the SMs or their descendants are necessary to mediate signals to the utse.

Discussion

Our results identify certain cellular (Fig. 10) and genetic requirements necessary for proper utse development. Using laser cell ablation, we identified four cell types in the environment of the utse that affect its development: the AC, ut1, ut2, and the SMs. We show that genes involved in AC invasion have a secondary role in promoting utse outgrowth. RNAi knockdown of two genes expressed in the uterine toroids, *rsef-1* and *unc-73,* show defects in utse development. *rsef-1* is a divergent Rab GTPase and we found that several Rab GTPases affect utse development, indicating that membrane trafficking may play a crucial role. Our results also show that *rho-1, unc-13,* and *unc-64* potentially act downstream of *unc-73.* We also see that *unc-53* plays a role in utse development through the SMs, and that the presence of SMs are necessary to maintain utse morphology.

Cell fusion and utse development

This study addressed the extent to which external cells affect the utse, and the role of cell fusion and subsequent internal signals on utse development. Transmission of genetic material between cells can change cell behavior, for instance cell fusion between differentiated cells and embryonic stem cells can induce pluripotency in the formerly differentiated cell (Tada et al. 2001). Specifically, we found that the AC, which fuses with the utse during L4, affects utse development. The AC nucleus is necessary for utse development, and the AC invasion genes *fos-1, cdh-3, egl-43, him-4, zmp-1,* and *mig-10* promote utse cell outgrowth.

rsef-1 and external cues in utse development

Surrounding tissues are known to have an impact on a cell's behavior and development for instance, *C. elegans* dorsal muscle cells express *slt-1*/Slit1 ligand to repel axons that express its corresponding receptor *sax-3*/Robo, and the ventrally expressed *unc-6*/Netrin ligand attracts axons that express its receptor *unc-40*/DCC/Frazzled (Killeen and Sybingco, 2008). Though we have determined that *rsef-1* and *unc-73* are expressed in the environment of the utse, we do not know the cells in which they function to affect utse development. The RASEF ortholog, *rsef-1*, is detectably expressed in the uterine toroids and it could act in the uterine toroids, the utse or both.

Rab GTPses and vesicular trafficking in uterine development

rsef-1 is computationally predicted to interact with other Rab GTPases (*rab-1* and *rab-11.1*) (Zhong and Sternberg, 2006). We showed that the predicted interactors *rab-1* and *rab-11.1,* and several other Rab GTPases (*rab-5, rab-6.2,* and *rab-10*) are required for proper utse development (Fig. 6, Table 2C). It is striking that we observe defects for multiple Rabs, which has not been the case in other *C. elegans* assays, suggesting that the utse development is sensitive to perturbations in membrane trafficking.

A potential role in the toroids could be that Rab GTPases are active in the uterine toroids and traffick cargo between the toroids to the utse. These Rab GTPases may deliver guidance cues to the utse that are necessary for development, or may deliver components of the extracellular matrix (ECM) to the growing utse. In some *C. elegans* tissues, Rab GTPase function has been found, but the cargo that these GTPases are transporting has not been identified. For instance, *rab-6.2* promotes vesicular transport necessary for grinder formation of *C. elegans*, yet its cargo is unknown (Straud et al., 2013). However, the Rab GTPases could also be transporting components of the extracellular matrix to the utse. For instance, *rab-11.1* has been characterized to deliver cortical granules containing chondroitin proteoglycans to the developing embryonic extracellular matrix (Sato et al., 2008). Rab GTPases can also transport guidance cues for utse cell outgrowth. Wnts are well-known guidance cues for cell and neuronal migration in *C. elegans* (Zinovyeva et al., 2008; Minor et al., 2013). RAB-7 is required for trafficking proteins that mediate Wnt

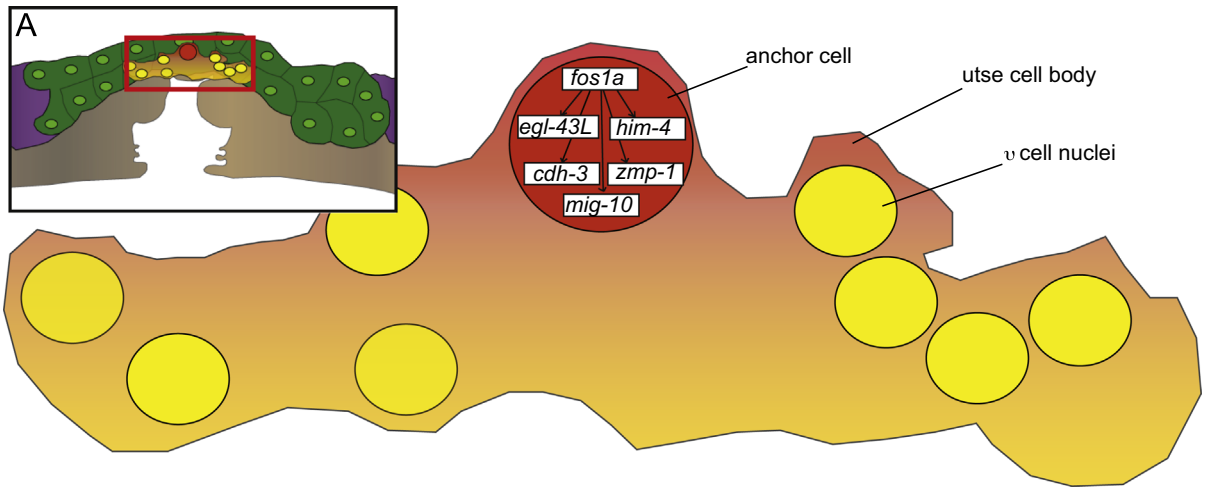

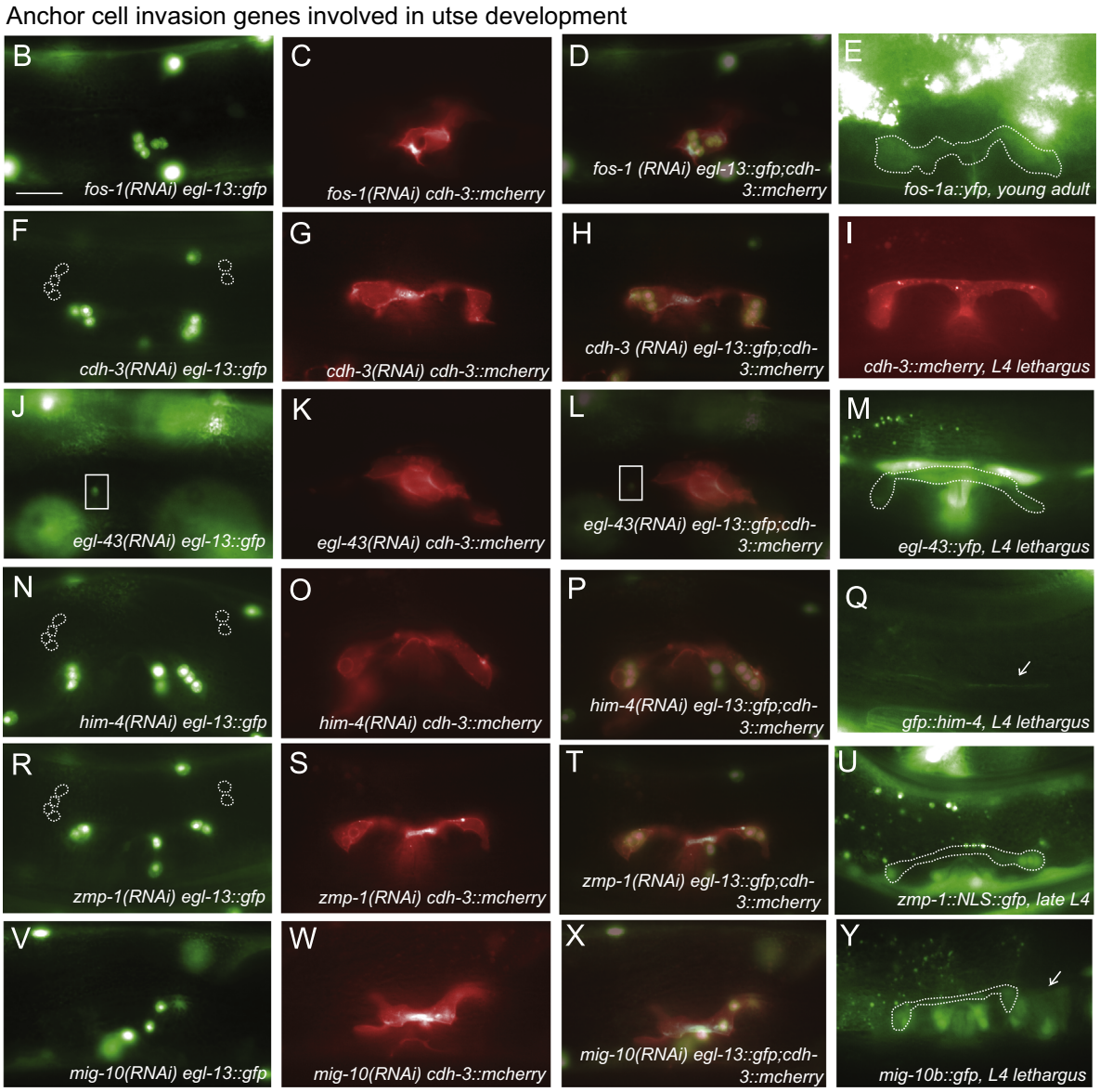

Fig. 6. AC invasion genes effects on utse development (A) Schematic of AC invasion genes. (B-D, F-H, J-L, N-P, R-T, V-X) utse cell body is marked with *cdh-3::mcherry* and nuclei are marked with *egl-13::gfp*. (F,N,R) cartoons show wild-type utse nuclei positions. (B-D) *fos-1*(*RNAi*) treated worms. (B,D) when π cells were induced, nuclei cluster and cease migrating. (C,D) cell body is misshaped. (E) *fos-1a* expression pattern, expressed in areas near the utse cell body at young adult (dashed lines show borders of expression). (F-H) *cdh-3*(*RNAi*) treated worms. (F, H) shorter nuclear migration. (G,H) cell body is misshapen and shorter. (I) *cdh-3* expression pattern, *cdh-3::mcherry* is expressed throughout the utse cell body. (J-L) *egl-43*(*RNAi*) treated worms. (J, L) υ cell is boxed, limited υ cell formation. (K,L) cell body is misshapen. (M) *egl-43* expression pattern. Faint expression in area around utse at L4 lethargus (dashed lines show borders of expression). (N-P) *him-4*(*RNAi*) treated worms. (N,P) shorter nuclear migration. (O,P) shorter cell body. (R) *him-4* expression pattern, expression in the basement membrane underneath utse. (R-T) *zmp-1*(*RNAi*) treated worms. (R,T) shorter nuclear migration. (S,T) shorter cell body. (U) *zmp-1* expression pattern, expression at late L4, localizes to υ cell nuclei. (V-X) *mig-10*(*RNAi*) treated worms. (V,X) misplaced and lower number of υ nuclei. (W-X) shorter and misshapen cell body. (Y) *mig-10* expression pattern. *mig-10* localizes to utse (see dashed border) and uterine toroids (see arrow). Scale bar, 100 μm.

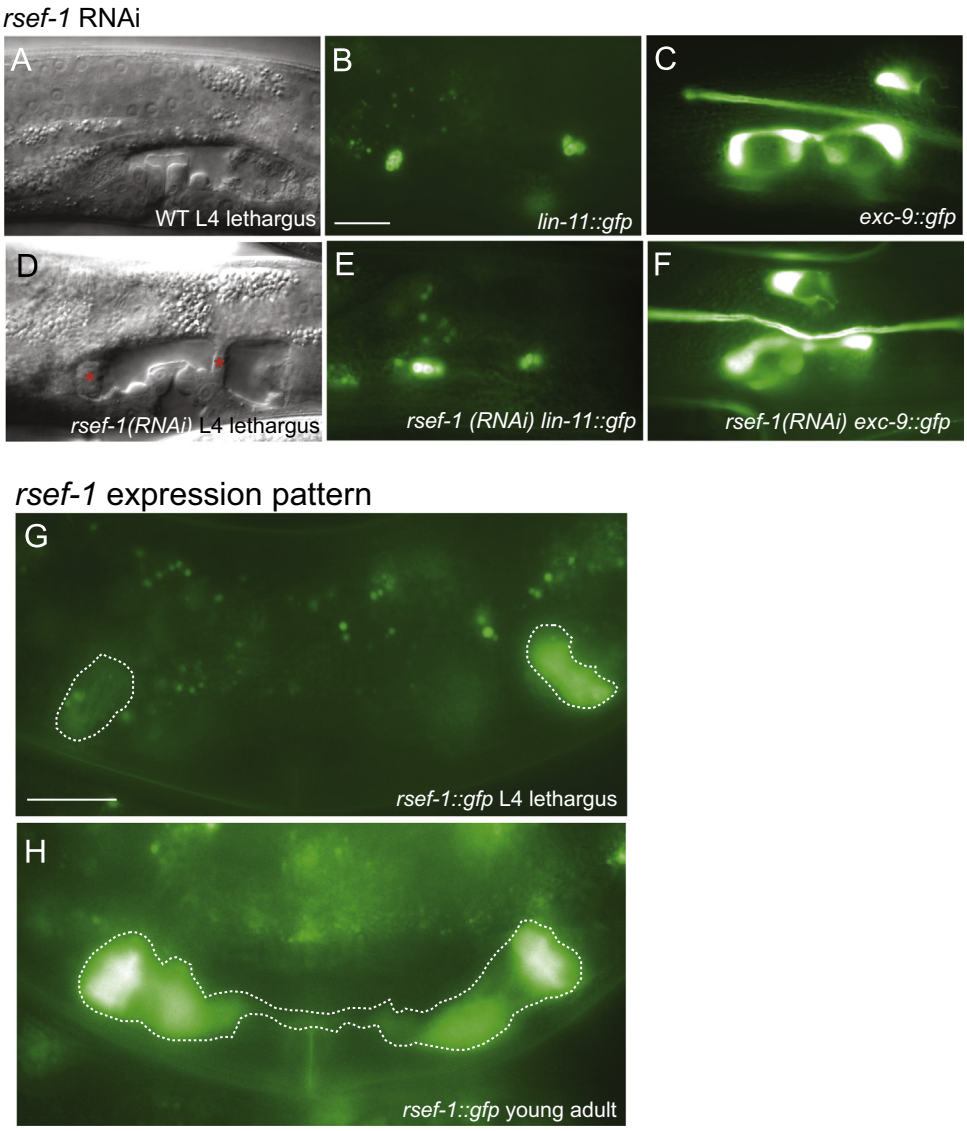

Fig. 7. *rsef-1* in utse development (A-F) utse cell body marked with *exc-9::gfp* and nuclei marked with *lin-11::gfp.* (A-C) Wild-type utse development. (A) wild-type L4 lethargus. (B) wild-type nuclear distance. (C) wild-type cell shape. (D-F) *rsef-1*(*RNAi*) treated worms. (D) problems in lumen formation in toroids (see asterisks). (E) reduced nuclear migration. (F) reduced cell outgrowth. (G-J) *rsef-1::gfp* expression. (G) *rsef-1* is expressed in the spermatheca at L4 lethargus. (H) *rsef-1* is expressed in the uterine toroids at young adult. Scale bar, 100 μm.

secretion (Wntless, Wls) between the endosome and trans-Golgi network which affects Wnt protein EGL-20 function (Lorenowicz et al., 2013). RAB-10 is involved in trafficking of glutamate receptors (Glodowski et al., 2007) and glutamate receptors are necessary for transducing signals for both proper neural cell outgrowth (Beraldo et al., 2011) and migrating neural progenitor cells (Castrén et al., 2005).

Trio, NAV and internal and external cues affecting the utse

The Trio RhoGNEF *unc-73* affects utse development and is expressed in the cell's environment as well as within the utse. Since we see *unc-73* expression within the utse, *unc-73* could lead to the modification of components of the ECM to promote proper utse outgrowth. *unc-73* is expressed within the Q neuroblasts and promotes protrusion formation within these cells (Dyer et al. 2010) through rearrangements of the actin cytoskeleton. *unc-73* is also expressed in the uterine toroids, and could be involved in the secretion of guidance cues between the uterine toroids and the utse. Evidence for this type of function has a precedent in *unc-73's* role in growth cone formation, for *unc-73* increases the ability of *slt-1* (slit) and *unc-6* (netrin) to influence posterior guidance cues (Hu et al., 2011; Watari-Goshima et al., 2007).

unc-73 acts with *unc-53* and *unc-71* to guide SM migration in a gonad-independent mechanism (Branda and Stern, 2000; Chen et al., 1997). This led us to discover a new role for *unc-53* in utse development. Since *unc-53* is solely expressed in the SMs, we ablated the SMs to determine their role in utse development and saw that they are necessary for maintaining proper utse cell shape and size. Since the SMs and their descendants flank the utse, we propose that the SMs or their descendants secrete a cue that helps maintain utse cell shape. One precedent for SMs providing a cue to surrounding tissues is their role in providing sources of Wnt to the vulval precursor cell P7.p (Minor et al. 2013). *unc-53* is a homolog of the human neuronal navigator genes NAV1, NAV2 and NAV3 (Maes et al., 2002), and promotes guidance in muscle, excretory cells and neuron, albeit in a cell autonomous manner (Stringham et al. 2002). Therefore, we propose a new non autonomous role for *unc-53* promoting utse outgrowth via the SMs.

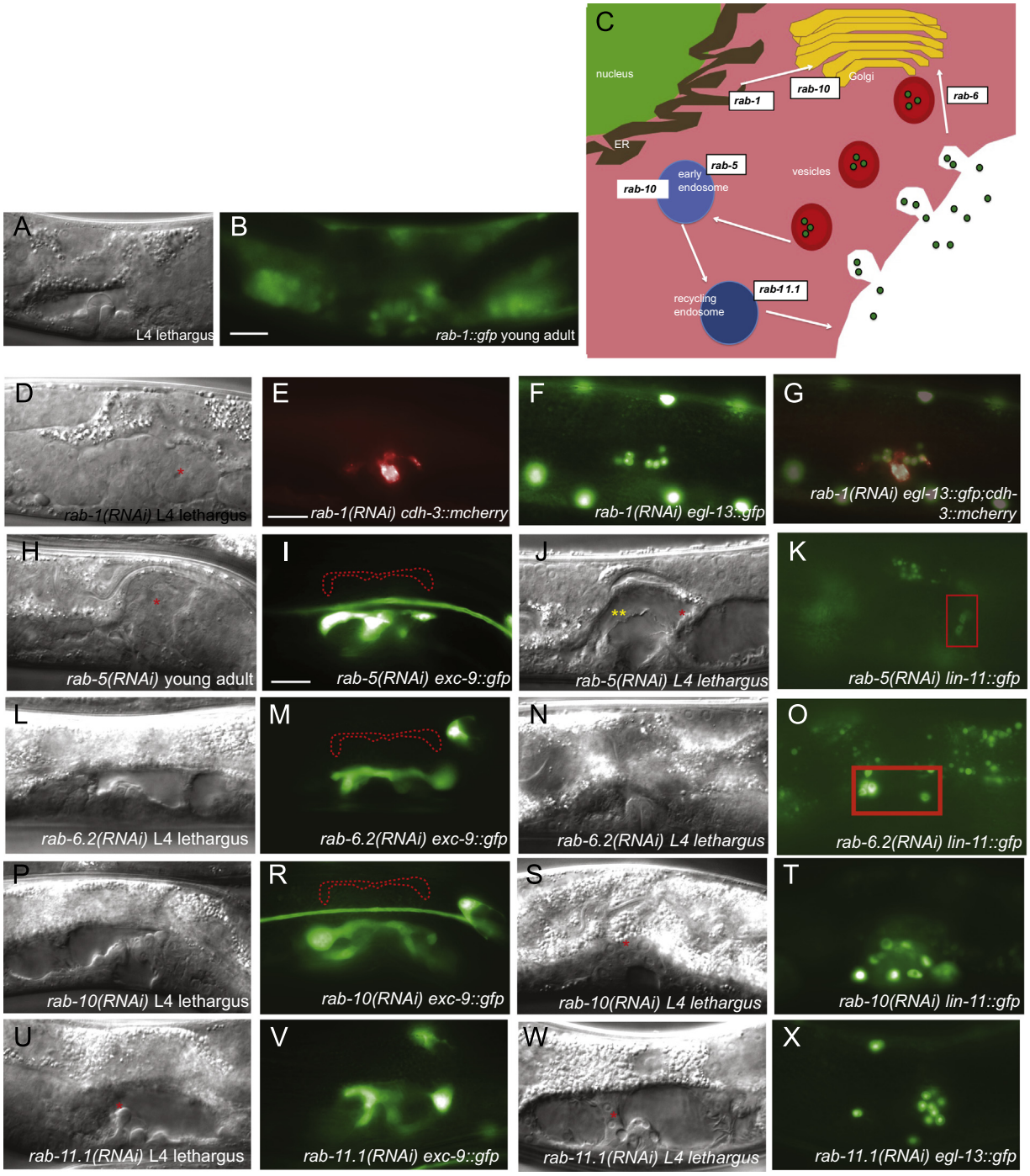

Fig. 8. RabGTPases in utse development (A,B) *rab-1* expression patterns at L4 lethargus in the uterine toroids. (C) Schematic of RabGTPases involved in utse development. (D-G) utse cell body is marked by *cdh-3::mcherry* and utse nuclei is marked by *egl-13::gfp*. *rab-1*(*RNAi*) treated worms (note *rab-1*(*RNAi*) treated worms grew three times slower than wild type, worms were staged based on vulval morphology and size). (D) stage for E-G. Uterine toroid lumen formation has not occurred (see red asterisk). (E, G) cell body is misshapen and no outgrowth has occurred. (F,G) nuclei have not migrated. (H-X) utse cell body marked with *exc-9::gfp* and utse nuclei are marked with *lin-11::gfp*. (I,M,R) dashed red cartoon indicates wild-type utse shape (H-K) *rab-5* (*RNAi*) treated worms. (H,J) stages for I and K were taken, respectively. Note in J, lumen formation has not occurred (see red asterisk) and and in K, part of utse has detached (see yellow asterisks). I) cell body missing sections. (K) nuclei are faint (see red box). (L-O) *rab-6.2* (*RNAi*) treated worms. (L,N) stages for M and O, respectively (M) cell body is misshapen. (O) shorter nuclear migration, nuclei contained in red box. (P-T) *rab-10* (*RNAi*) treated worms. (P,S) stages for R and T, respectively. Note in S, problems in lumen formation are present (see red asterisk). (R) cell body is misshapen. (T) nuclei are clustered. (U-X) *rab-11.1* (*RNAi*) treated worms. (U,W) stages for V and X, respectively. Bleb formed in cell membrane in U and defective lumen formation are present in W (see red asterisks). (V) cell body is shorter and missing parts. (X) shorter nuclear migration. Scale bar, 100 μm.

Broad implications of identification of utse genetic inputs

A variety of cell biological systems and disease models use mechanisms that function in utse development. Several of the genes identified, such as *unc-73* and *unc-53*, are key growth cone regulators, indicating that the utse could be used as a model to study genes involved in neurite outgrowth. RabGTPases are well characterized in several migratory systems, and the number of Rabs found in the utse makes it an excellent system for studying these GTPases.

Since the utse and the synctiotrophoblast layer of the placenta (Cross, 2000) are both syncytia, the utse can act as a potential model to study morphogenetic movements in this system.

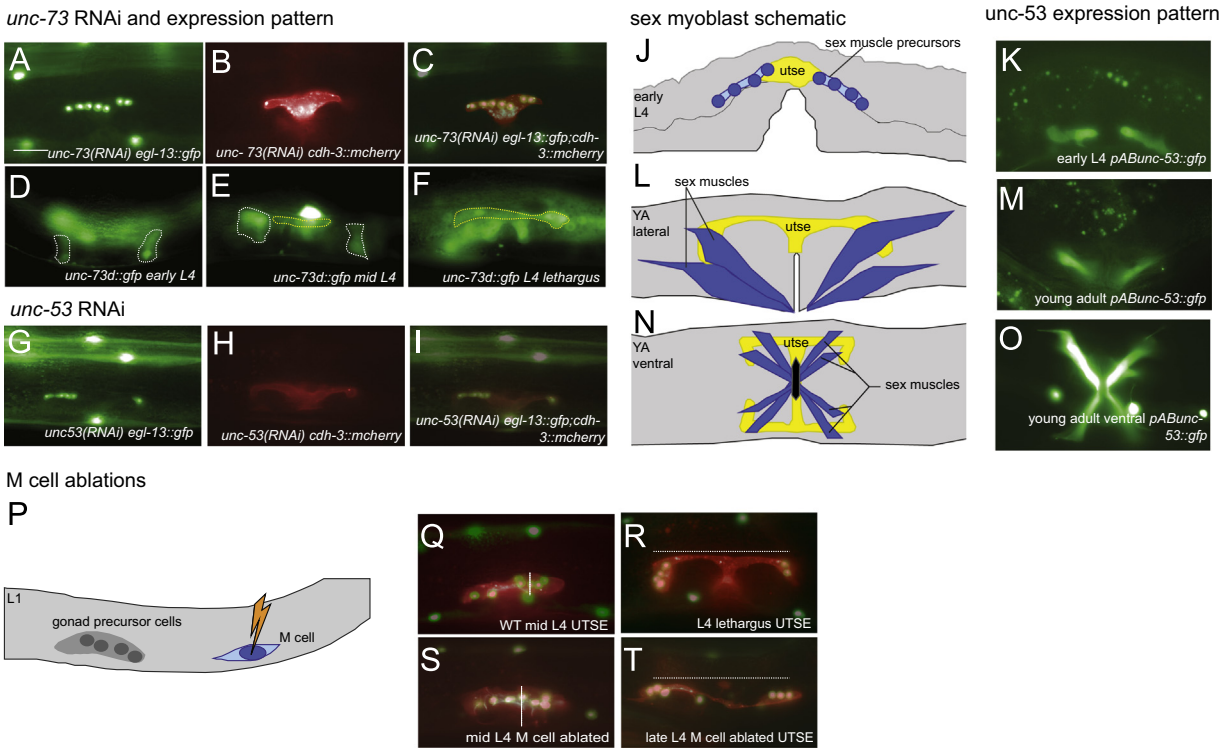

Fig. 9. *unc-73, unc-53* and SMs in utse development (A-C; G-I) utse cell body marked with *cdh-3::mcherry* and nuclei marked with *egl-13::gfp*. (A-C) *unc-73*(*RNAi*) treated worms. (B,C) nuclei have not segregated into two groups or migrated. (B,C) cell body is thick and misshapen. (D-F) *unc-73d::gfp* pattern. (D) expression in early L4, white dashed lines indicate ut2 expression. (E) expression in mid L4, white dashed lines show ut1 and ut2 expression and yellow dashed lines show utse expression. (F) expression in L4 lethargus worms, yellow dashed lines show utse expression. (G-I) *unc-53*(*RNAi*) treated worms. (G,I), nuclei are arranged linearly (similar to utse nuclei in *unc-73*(*RNAi*) treated worms), and have defective migration. (H,I) cell body is thick and misshapen also similar to *unc-73*(*RNAi*) treated worms. (J, L, N) schematics showing different stages of sex myoblast (SM) development. (K, M, O) *pABunc-53::gfp* expression pattern. (J) sex myoblast position at early L4. (K) *unc-53* expression in sex myoblasts. (L) lateral view of sex muscles in young adult. (M) *unc-53* expression in sex muscles (vulval muscles shown, uterine muscle expression in separate plane, not shown). (N) ventral view of sex muscles in young adult. (O) *unc-53* expression in sex muscles. (P) schematic of M cell (SM precursor) ablation at L1. (Q-T) utse cell body marked with *cdh-3::mcherry* and nuclei marked with *egl-13::gfp*. (Q-R) wild-type utse development. (Q) mid L4 utse, vertical dashed line shows widest point of utse. (R) L4 lethargus utse, horizontal dashed line shows wild-type length. (S) mid L4 utse in M cell ablated worm. utse is wider (see vertical dashed line at widest point). (T) late L4 utse in M cell ablated worm, utse is longer (see horizontal dashed line for comparison to wild-type length). Scale bar, 100 μm.

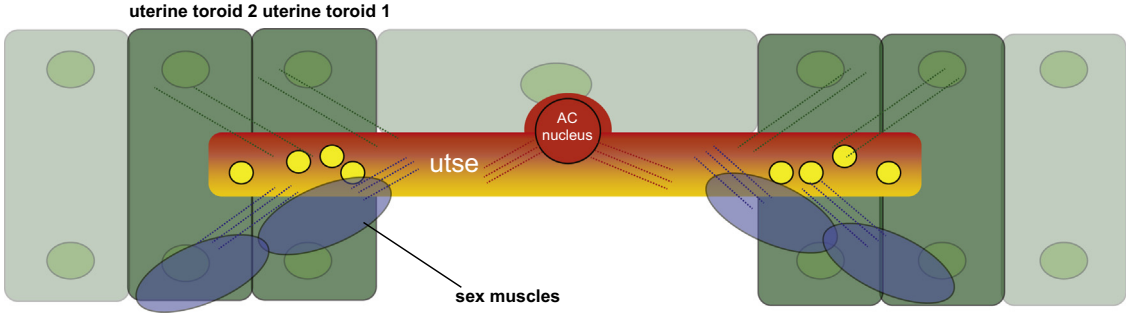

Fig. 10. Mechanisms involved in utse development. Schematic of different cells influencing utse development at mid L4. Dashed lines indicate signals generated from cells that affect utse development. ut1, ut2 and SMs generate external signals. The AC generates internal signals.

Extravillious trophoblast (EVT) tissue invades the synctiotrophoblast and RhoA is necessary for migration of EVT (Nicola et al., 2008). Here have shown that *rho-1*, a homolog of RhoA, is involved in utse outgrowth, illustrating the potential to use the utse as a model to study factors involved in placental development. Poor placental formation can deplete the fetus of nutrition, causing birth defects, and can cause in preeclampsia, indicating a need for study of this tissue.

Metastatic cancers also use several of the mechanisms that function in utse development. The *unc-73* homolog Trio is involved with the migration and invasiveness of glioblastoma cells (Fortin et al., 2012) and in breast cancer cell metastasis (Li et al., 2011). Alterations of NAV3 an ortholog of *unc-53,* are characteristic of colorectal cancer cells (Carlsson et al., 2012) and certain Rab GTPases are upregulated in ovarian and breast cancer (Cheng et al., 2005). The utse grows outwards in a manner similar to that of metastatic cancer cells (through rearranging its cytoskeleton and changing from an ellipsoid to a linear shape.) Therefore, the *C. elegans* utse may serve as a new model to understand the normal function of genes implicated in metastatic cell behavior.

Acknowledgments

We thank Matthew Buechner (University of Kansas), David Sherwood (Duke University), Ian Hope (University of Leeds),

Nathalie Pujol (Centre d'Immunologie de Marseille-Luminy) and the Caenorhabditis Genetics Center (University of Minnesota) for worm strains; Sang Nguyen for verification of uterine toroid genes; Barbara Perry and Gladys Medina for technical assistance; Wendy Hanna-Rose, Marianne Bronner, Bruce Hay, David Chan, Amir Sapir, Mihoko Kato, Paul Minor and Hillel Schwartz for helpful discussions and critically reading the manuscript. S.G. was supported by National Institutes of Health USPHS training grant GM07616. This work was supported by the Howard Hughes Medical Institute, with which P.W.S. is an investigator.

Appendix A. Supporting information

Supplementary data associated with this article can be found in the online version at http://dx.doi.org/10.1016/j.ydbio.2014.09.028.

References

Bargmann, C.I., Avery, L., 1995. Laser killing of cells in *Caenorhabditis elegans*. Methods Cell Biol. 48, 225–250.
Beraldo, F.H., Arantes, C.P., Santos, T.G., Machado, C.F., Roffe, M., Hajj, G.N., Lee, K.S., Magalhães, A.C., Caetano, F.A., Mancini, G.L., Lopes, M.H., Américo, T.A., Magdesian, M.H., Ferguson, S.S., Linden, R., Prado, M.A., Martins, V.R., 2011. Metabotropic glutamate receptors transduce signals for neurite outgrowth after binding of the prion protein to laminin γ1 chain. FASEB J 25, 265–279.
Berndt, B., Zänker, K.S., Dittmar, T., 2013. Cell fusion is a potent inducer of aneuploidy and drug resistance in tumor cell/normal cell hybrids. Crit. Rev. Oncog. 18, 97–113.
Biressi, S., Tagliafico, E., Lamorte, G., Monteverde, S., Tenedini, E., Roncaglia, E., Ferrari, S., Ferrari, S., Cusella-De Angelis, M.G., Tajbakhsh, S., Cossu, G., 2007. Intrinsic phenotypic diversity of embryonic and fetal myoblasts is revealed by genome-wide gene expression analysis on purified cells. Dev. Biol. 304, 633–651.
Branda, C.S., Stern, M.J., 2000. Mechanisms controlling sex myoblast migration in *Caenorhabditis elegans* hermaphrodites. Dev Biol. 226, 137–151.
Brenner, S., 1974. The genetics of Caenorhabditis elegans. Genetics 77, 71–94.
Bronner, M.E., LeDouarin, N.M., 2011. Development and evolution of the neural crest: an overview. Dev. Biol. 366, 2–9.
Carlsson, E., Ranki, A., Sipilä, L., Karenko, L., Abdel-Rahman, W.M., Ovaska, K., Siggberg, L., Aapola, U., Ässämäki, R., Häyry, V., Niiranen, K., Helle, M., Knuutila, S., Hautaniemi, S., Peltomäki, P., Krohn, K., 2012. Potential role of a navigator gene NAV3 in colorectal cancer. Br. J. Cancer. 106, 517–524.
Cajal, S., Ramón, y., 1890. A quelle epoque apparaissent les expansions des cellules nerveuses de la moëlle épinière du poulet? Anat. Anz 5, 609–613 631-639.
Castrén, M., Tervonen, T., Kärkkäinen, V., Heinonen, S., Castrén, E., Larsson, K., Bakker, C.E., Oostra, B.A., Akerman, K., 2005. Altered differentiation of neural stem cells in fragile X syndrome. Proc. Natl. Acad. Sci. USA 102, 17834–17839.
Chamberlin, H.M., Palmer, R.E., Newman, A.P., Sternberg, P.W., Baillie, D.L., Thomas, J.H., 1997. The PAX gene egl-38 mediates developmental patterning in Caenorhabditis elegans. Development 124, 3919–3928.
Chang, C., Newman, A.P., Sternberg, P.W., 1999. Reciprocal EGF signaling back to the uterus from the induced *C. elegans* vulva coordinates morphogenesis of epithelia. Curr. Biol. 9, 237–246.
Chen, E.B., Branda, C.S., Stern, M.J., 1997. Genetic enhancers of sem-5 define components of the gonad-independent guidance mechanism controlling sex myoblast migration in *Caenorhabditis elegans* hermaphrodites. Dev. Biol. 182, 88–100.
Chen, L., Wang, Z., Ghosh-Roy, A., Hubert, T., Yan, D., O'Rourke, S., Bowerman, B., Wu, Z., Jin, Y., Chisholm, A.D., 2011. Axon regeneration pathways identified by systematic genetic screening in *C. elegans*. Neuron 71, 1043–1057.
Chen, Y.T., Holcomb, C., Moore, H.P., 1993. Expression and localization of two low molecular weight GTP-binding proteins, Rab8 and Rab10, by epitope tag. Proc. Natl. Acad. Sci. USA 90, 6508–6512.
Cheng, K.W., Lahad, J.P., Gray, J.W., Mills, G.B., 2005. Emerging role of RAB GTPases in cancer and human disease. Cancer Res. 65, 2516–2519.
Cinar, H.N., Richards, K.L., Oommen, K.S., Newman, A.P., 2003. The EGL-13 SOX domain transcription factor affects the uterine pi cell lineages in *Caenorhabditis elegans*. Genetics 165, 1623–1628.
Cross, J.C., 2000. Genetic insights into trophoblast differentiation and placental morphogenesis. Semin. Cell Dev. Biol. 11, 105–113.
Daigle, S.N., Creutz, C.E., 1999. Transcription, biochemistry and localization of nematode annexins. J. Cell Sci. 112, 1901–1913.
Dyer, J.O., Demarco, R.S., Lundquist, E.A., 2010. Distinct roles of Rac GTPases and the UNC-73/Trio and PIX-1 Rac GTP exchange factors in neuroblast protrusion and migration in *C. elegans*. Small GTPases 1, 44–61.
Félix, M.A., Sternberg, P.W., 1996. Symmetry breakage in the development of one-armed gonads in nematodes. Development 122, 2129–2142.
Fortin, S.P., Ennis, M.J., Schumacher, C.A., Zylstra-Diegel, C.R., Williams, B.O., Ross, J.T., Winkles, J.A., Loftus, J.C., Symons, M.H., Tran, N.L., 2012. Cdc42 and the guanine nucleotide exchange factors Ect2 and trio mediate Fn14-induced migration and invasion of glioblastoma cells. Mol. Cancer Res. 10, 958–968.
Gabbiani, G., Ryan, G.B., Majno, G., 1971. Presence of modified fibroblasts in granulation tissue and their possible role in wound contraction. Experientia 27, 549–550.
Gabbiani, G., 2003. The myofibroblast in wound healing and fibrocontractive diseases. J. Pathol. 200, 500–503.
Glodowski, D.R., Chen, C.C., Schaefer, H., Grant, B.D., Rongo, C., 2007. RAB-10 regulates glutamate receptor recycling in a cholesterol-dependent endocytosis pathway. Mol. Biol. Cell. 18, 4387–4396.
Gomez, T.M., Zheng, J.Q., 2006. The molecular basis for calcium-dependent axon pathfinding. Nat. Rev. Neurosci. 7, 115–125.
Grinnell, F., 1992. Wound repair, keratinocyte activation and integrin modulation. J. Cell Sci. 101, 1–5.
Hall, B.K., 2009. The Neural Crest and Neural Crest Cells in Vertebrate Development and Evolution. Springer, New York, NY.
Hanna-Rose, W., Han, M., 1999. COG-2, a sox domain protein necessary for establishing a functional vulval-uterine connection in Caenorhabditis elegans. Development 126, 169–179.
Hedgecock, E.M., Culotti, J.G., Hall, D.H., Stern, B.D., 1987. Genetics of cell and axon migrations in Caenorhabditis elegans. Development 100, 365–382.
Hedgecock, E.M., Culotti, J.G., Hall, D.H., 1990. The unc-5, unc-6, and unc-40 genes guide circumferential migrations of pioneer axons and mesodermal cells on the epidermis in *C. elegans*. Neuron 4, 61–85.
Hill, R.J., Sternberg, P.W., 1992. The gene lin-3 encodes an inductive signal for vulval development in *C. elegans*. Nature 358, 470–4776.
Hristova, M., Birse, D., Hong, Y., Ambros, V., 2005. The Caenorhabditis elegans heterochronic regulator LIN-14 is a novel transcription factor that controls the developmental timing of transcription from the insulin/insulin-like growth factor gene ins-33 by direct DNA binding. Mol. Cell Biol. 25, 11059–11072.
Hu, S., Pawson, T., Steven, R.M., 2011. UNC-73/trio RhoGEF-2 activity modulates *Caenorhabditis elegans* motility through changes in neurotransmitter signaling upstream of the GSA-1/Galphas pathway. Genetics 189, 137–151.
Huang, L., Hanna-Rose, W., 2006. EGF signaling overcomes a uterine cell death associated with temporal mis-coordination of organogenesis within the *C. elegans* egg-laying apparatus. Dev. Biol. 300, 599–611.
Hwang, B.J., Sternberg, P.W., 2004. A cell-specific enhancer that specifies lin-3 expression in the *C. elegans* anchor cell for vulval development. Development 131, 143–151.
Hwang, B.J., Meruelo, A.D., Sternberg, P.W., 2007. C. elegans EVI1 proto-oncogene, EGL-43, is necessary for Notch-mediated cell fate specification and regulates cell invasion. Development 134, 669–679.
Ihara, S., Hagedorn, E.J., Morrissey, M.A., Chi, Q., Motegi, F., Kramer, J.M., Sherwood, D.R., 2011. Basement membrane sliding and targeted adhesion remodels tissue boundaries during uterine-vulval attachment in Caenorhabditis elegans. Nat. Cell Biol. 13, 669–679.
Ishii, N., Wadsworth, W.G., Stern, B.D., Culotti, J.G., Hedgecock, E.M., 1992. UNC-6, a laminin-related protein, guides cell and pioneer axon migrations in *C. elegans*. Neuron 9, 873–881.
Kadam, S., Ghosh, S., Stathopoulos, A., 2012. Synchronous and symmetric migration of Drosophila caudal visceral mesoderm cells requires dual input by two FGF ligands. Development 139, 699–708.
Kato, M., Sternberg, P.W., 2009. The *C. elegans* tailless/Tlx homolog nhr-67 regulates a stage-specific program of linker cell migration in male gonadogenesis. Development 136, 3907–3915.
Kemp, K., Gray, E., Wilkins, A., Scolding, N., 2012. Purkinje cell fusion and binucleate heterokaryon formation in multiple sclerosis cerebellum. Brain 135, 2962–2972.
Killeen, M.T., Sybingco, S.S., 2008. Netrin, Slit and Wnt receptors allow axons to choose the axis of migration. Dev. Biol. 323, 143–151.
Kimble, J., Hirsh., D., 1979. The postembryonic cell lineages of the hermaphrodite and male gonads in *Caenorhabditis elegans*. Dev. Biol. 70, 396–417.
Kubiseski, T.J., Culotti, J., Pawson, T., 2003. Functional analysis of the *Caenorhabditis elegans* UNC-73B PH domain demonstrates a role in activation of the Rac GTPase in vitro and axon guidance in vivo. Mol Cell. Biol. 23, 6823–6835.
Lackner, M.R., Nurrish, S.J., Kaplan, J.M., 1999. Facilitation of synaptic transmission by EGL-30 Gqalpha and EGL-8 PLCbeta: DAG binding to UNC-13 is required to stimulate acetylcholine release. Neuron 24, 335–346.
Le Douarin, N.M., Kalcheim, C., 1999. The Neural Crest. Cambridge University Press, Cambridge, United Kingdom.
Li, Y., Guo, Z., Chen, H., Dong, Z., Pan, Z.K., Ding, H., Su, S.B., Huang, S., 2011. HOXC8-Dependent Cadherin 11 Expression Facilitates Breast Cancer Cell Migration through Trio and Rac. Genes Cancer 2, 880–888.
Lorenowicz, M.J., Macurkova, M., Harterink, M., Middelkoop, T.C., de Groot, R., Betist, M.C., Korswagen, H.C., 2013. Inhibition of late endosomal maturation restores Wnt secretion in *Caenorhabditis elegans* vps-29 retromer mutants. Cell Signal. 26, 19–31.
Maes, T., Barceló, A., Buesa, C., 2002. Neuron navigator: a human gene family with homology to unc-53, a cell guidance gene from *Caenorhabditis elegans*. Genomics 80, 21–30.
Marcus-Gueret, N., Schmidt, K.L., Stringham, E.G., 2012. Distinct cell guidance pathways controlled by the Rac and Rho GEF domains of UNC-73/TRIO in Caenorhabditis elegans. Genetics 190, 129–142.
Martin, P., 1997. Wound healing–aiming for perfect skin regeneration. Science 276, 75–81.

Martin, P., Leibovich, S.J., 2005. Inflammatory cells during wound repair: the good, the bad and the ugly. Trends Cell Biol. 15, 599–607.
Martinez, O., Schmidt, A., Salaméro, J., Hoflack, B., Roa, M., Goud, B., 1994. The small GTP-binding protein rab6 functions in intra-Golgi transport. J. Cell. Biol. 127, 1575–1588.
McMullan, R., Hiley, E., Morrison, P., Nurrish, S.J., 2006. Rho is a presynaptic activator of neurotransmitter release at pre-existing synapses in *C. elegans*. Genes Dev. 20, 65–76.
Minor, P.J., He, T.F., Sohn, C.H., Asthagiri, A.R., Sternberg, P.W., 2013. FGF signaling regulates Wnt ligand expression to control vulval cell lineage polarity in *C. elegans*. Development 140, 3882–3891.
Mounsey, A., Bauer, P., Hope, I.A., 2002. Evidence suggesting that a fifth of annotated Caenorhabditis elegans genes may be pseudogenes. Genome Res. 12, 770–775.
Newman, A.P., White, J.G., Sternberg, P.W., 1995. The Caenorhabditis elegans lin-12 gene mediates induction of ventral uterine specialization by the anchor cell. Development 121, 263–271.
Newman, A.P., White, J.G., Sternberg, P.W., 1996. Morphogenesis of the *C. elegans* hermaphrodite uterus. Development 122, 3617–3626.
Newman, A.P., Acton, G.Z., Hartwieg, E., Horvitz, H.R., Sternberg, P.W., 1999. The lin-11 LIM domain transcription factor is necessary for morphogenesis of *C. elegans* uterine cells. Development 126, 5319–5326.
Nicola, C., Chirpac, A., Lala, P.K., Chakraborty, C., 2008. Roles of Rho guanosine 5'-triphosphatase A, Rho kinases, and extracellular signal regulated kinase (1/2) in prostaglandin E2-mediated migration of first-trimester human extravillous trophoblast. Endocrinology 149, 1243–1251.
Nishimura, N., Sasaki, T., 2008. Regulation of epithelial cell adhesion and repulsion: role of endocytic recycling. J. Med. Invest. 55, 9–16.
Oommen, K.S., Newman, A.P., 2007. Co-regulation by Notch and Fos is required for cell fate specification of intermediate precursors during *C. elegans* uterine development. Development 134, 3999–4009.
Oshita, H., Nishino, R., Takano, A., Fujitomo, T., Aragaki, M., Kato, T., Akiyama, H., Tsuchiya, E., Kohno, N., Nakamura, Y., Daigo, Y., 2013. RASEF is a novel diagnostic biomarker and a therapeutic target for lung cancer. Mol. Cancer Res. 11, 937–951.
Pignoni, F., Baldarelli, R.M., Steingrímsson, E., Diaz, R.J., Patapoutian, A., Merriam, J.R., Lengyel, J.A., 1990. The Drosophila gene tailless is expressed at the embryonic termini and is a member of the steroid receptor superfamily. Cell 62, 151–163.
Podbilewicz, B., Leikina, E., Sapir, A., Valansi, C., Suissa, M., Shemer, G., Chernomordik, L.V., 2006. The *C. elegans* developmental fusogen EFF-1 mediates homotypic fusion in heterologous cells and in vivo. Dev. Cell. 11, 471–481.
Rimann, I., Hajnal, A., 2007. Regulation of anchor cell invasion and uterine cell fates by the egl-43 Evi-1 proto-oncogene in *Caenorhabditis elegans*. Dev. Biol. 2007 (308), 187–195.
Robertson, T.A., Grounds, M.D., Mitchell, C.A., Papadimitriou, J.M., 1990. Fusion between myogenic cells in vivo: an ultrastructural study in regenerating murine skeletal muscle. J. Struct. Biol. 105, 170–182.
Robertson, T.A., Maley, M.A., Grounds, M.D., Papadimitriou, J.M., 1993. The role of macrophages in skeletal muscle regeneration with particular reference to chemotaxis. Exp. Cell Res. 207, 321–331.
Rutledge, E., Denton, J., Strange, K., 2002. Cell cycle- and swelling-induced activation of a *Caenorhabditis elegans* ClC channel is mediated by CeGLC-7alpha/beta phosphatases. J. Cell Biol. 158, 435–444.
Saleh, M.C., van Rij, R.P., Hekele, A., Gillis, A., Foley, E., O'Farrell, P.H., Andino, R., 2006. The endocytic pathway mediates cell entry of dsRNA to induce RNAi silencing. Nat. Cell Biol. 8, 793–802.
Sapir, A., Choi, J., Leikina, E., Avinoam, O., Valansi, C., Chernomordik, L.V., Newman, A.P., Podbilewicz, B., 2007. AFF-1, a FOS-1-regulated fusogen, mediates fusion of the anchor cell in *C. elegans*. Dev. Cell 12, 683–698.
Sato, M., Grant, B.D., Harada, A., Sato, K., 2008. Rab11 is required for synchronous secretion of chondroitin proteoglycans after fertilization in *Caenorhabditis elegans*. J. Cell Sci. 12, 3177–3186.
Satoh, A., Miwa, H.E., Kojima, K., Hirabayashi, J., Matsumoto, I., 2000. Ligand-binding properties of annexin from *Caenorhabditis elegans* (annexin XVI, Nex-1). J. Biochem. 128, 377–381.
Schmidt, K.L., Marcus-Gueret, N., Adeleye, A., Webber, J., Baillie, D., Stringham, E.G., 2009. The cell migration molecule UNC-53/NAV2 is linked to the ARP2/3 complex by ABI-1. Development 136, 563–574.
Schuurs, T.A., Dalstra, H.J., Scheer, J.M., Wessels, J.G., 1998. Positioning of nuclei in the secondary Mycelium of Schizophyllum commune in relation to differential gene expression. Fungal Genet. Biol. 23, 150–161.
Seipel, K., Medley, Q.G., Kedersha, N.L., Zhang, X.A., O'Brien, S.P., Serra-Pages, C., Hemler, M.E., Streuli, M., 1999. Trio amino-terminal guanine nucleotide exchange factor domain expression promotes actin cytoskeleton reorganization, cell migration and anchorage-independent cell growth. J. Cell Sci. 112, 1825–1834.
Shaye, D.D., Greenwald, I., 2011. OrthoList: a compendium of *C. elegans* genes with human orthologs. PLoS One 6, e20085.
Sherwood, D.R., Sternberg, P.W., 2003. Anchor cell invasion into the vulval epithelium in *C. elegans*. Dev. Cell. 5, 21–31.
Sherwood, D.R., Butler, J.A., Kramer, J.M., Sternberg, P.W., 2005. FOS-1 promotes basement-membrane removal during anchor-cell invasion in *C. elegans*. Cell 121, 951–962.
Siddiqui, S.S., 1990. Mutations affecting axonal growth and guidance of motor neurons and mechanosensory neurons in the nematode *Caenorhabditis elegans*. Neurosci. Res. 13, S171–S190.
Spencer, A.G., Orita, S., Malone, C.J., Han, M., 2001. A RHO GTPase-mediated pathway is required during P cell migration in *Caenorhabditis elegans*. Proc. Natl. Acad. Sci USA 98, 13132–13137.
Steven, R., Kubiseski, T.J., Zheng, H., Kulkarni, S., Mancillas, J., Ruiz Morales, A., Hogue, C.W., Pawson, T., Culotti, J., 1998. UNC-73 activates the Rac GTPase and is required for cell and growth cone migrations in *C. elegans*. Cell 92, 785–795.
Steven, R., Zhang, L., Culotti, J., Pawson, T., 2005. The UNC-73/Trio RhoGEF-2 domain is required in separate isoforms for the regulation of pharynx pumping and normal neurotransmission in *C. elegans*. Genes. Dev. 19, 2016–2029.
Straud, S., Lee, I., Song, B., Avery, L., You, Y.J., 2013. The jaw of the worm: GTPase-activating protein EAT-17 regulates grinder formation in *Caenorhabditis elegans*. Genetics 195, 115–125.
Stringham, E., Pujol, N., Vandekerckhove, J., Bogaert, T., 2002. unc-53 controls longitudinal migration in *C. elegans*. Development 129, 3367–3379.
Sulston, J.E., Horvitz, H.R., 1977. Post-embryonic cell lineages of the nematode, *Caenorhabditis elegans*. Dev. Biol. 56, 110–156.
Tada, M., Takahama, Y., Abe, K., Nakatsuji, N., Tada, T., 2001. Nuclear reprogramming of somatic cells by in vitro hybridization with ES cells. Curr. Biol. 11, 1553–1558.
Theveneau, E., Mayor, R., 2012. Neural crest delamination and migration: from epithelium-to-mesenchyme transition to collective cell migration. Dev. Biol. 366, 34–54.
Timmons, L., Court, D.L., Fire, A., 2001. Ingestion of bacterially expressed dsRNAs can produce specific and potent genetic interference in *Caenorhabditis elegans*. Gene 263, 103–112.
Tong, X., Buechner, M., 2008. CRIP homologues maintain apical cytoskeleton to regulate tubule size in *C. elegans*. Dev Biol. 317, 225–233.
Vitriol, E.A., Zheng, J.Q., 2012. Growth cone travel in space and time: the cellular ensemble of cytoskeleton, adhesion, and membrane. Neuron 73, 1068–1081.
Vogel, B.E., Muriel, J.M., Dong, C., Xu, X., 2006. Hemicentins: what have we learned from worms? Cell Res. 16, 872–878.
Wang, Z., Chi, Q., Sherwood, D.R., 2014. MIG-10 (lamellipodin) has netrin-independent functions and is a FOS-1A transcriptional target during anchor cell invasion in *C. elegans*. Development 141, 1342–1353.
Watari-Goshima, N., Ogura, K., Wolf, F.W., Goshima, Y., Garriga, G., 2007. *C. elegans* VAB-8 and UNC-73 regulate the SAX-3 receptor to direct cell and growth-cone migrations. Nat. Neurosci. 10, 169–176.
Wightman, B., Baran, R., Garriga, G., 1997. Genes that guide growth cones along the *C. elegans* ventral nerve cord. Development 124, 2571–2580.
Wormbase website, 2014, ⟨http://www.wormbase.org⟩/species/c_elegans/gene/WBGene00016344?query=tag-312#0c-9d1b6-10, release WS241.
Wu, Y.C., Cheng, T.W., Lee, M.C., Weng, N.Y., 2002. Distinct rac activation pathways control *Caenorhabditis elegans* cell migration and axon outgrowth. Dev. Biol. 250, 145–155.
Youds, J.L., Barber, L.J., Ward, J.D., Collis, S.J., O'Neil, N.J., Boulton, S.J., Rose, A.M., 2007. DOG-1 is the *Caenorhabditis elegans* BRIP1/FANCJ homologue and functions in interstrand cross-link repair. Mol. Cell Biol. 28, 1470–1479.
Zhang, C.L., Zou, Y., He, W., Gage, F.H., Evans, R.M., 2008. A role for adult TLX-positive neural stem cells in learning and behaviour. Nature 7181, 1004–1007.
Zhong, W., Sternberg, P.W., 2006. Genome-wide prediction of *C. elegans* genetic interactions. Science 311, 1481–1484.
Ziel, J.W., Matus, D.Q., Sherwood, D.R., 2009. An expression screen for RhoGEF genes involved in *C. elegans* gonadogenesis. Gene Expr. Patterns. 9, 397–403.
Zinovyeva, A.Y., Yamamoto, Y., Sawa, H., Forrester, W.C., 2008. Complex network of Wnt signaling regulates neuronal migrations during *Caenorhabditis elegans* development. Genetics 179, 1357–1371.